ENERGY RESEARCH AND DEVELOPMENT DIVISION

FINAL PROJECT REPORT

Performance-Based Earthquake Engineering Assessment Tool for Gas Storage and Pipeline Systems

PREPARED BY:

Jonathan Bray and Norman Abrahamson
University of California at Berkeley
Primary Authors

Jennie Watson-Lamprey and Micaela Largent
Slate Geotechnical Consultants, Inc.

Yahui Yang
Project Manager
California Energy Commission

Agreement Number: PIR-18-003

Reynaldo Gonzalez
Branch Manager
Energy Systems & Transportation Branch

Jonah Steinbuck, Ph.D.
Director
ENERGY RESEARCH AND DEVELOPMENT DIVISION

Drew Bohan
Executive Director

ACKNOWLEDGEMENTS

PREFACE

The California Energy Commission's (CEC) Energy Research and Development Division manages the Gas Research and Development Program, which supports energy-related research, development, and demonstration not adequately provided by competitive and regulated markets. These natural gas research investments spur innovation in energy efficiency, renewable energy and advanced clean generation, energy-related environmental protection, energy transmission and distribution and transportation.

The Energy Research and Development Division conducts this public interest natural gas-related energy research by partnering with RD&D entities, including individuals, businesses, utilities, and public and private research institutions. This program promotes greater gas reliability, lower costs, and increased safety for Californians and is focused in these areas:

- Buildings End-Use Energy Efficiency

- Industrial, Agriculture and Water Efficiency

- Renewable Energy and Advanced Generation

- Natural Gas Infrastructure Safety and Integrity

- Energy-Related Environmental Research

- Natural Gas-Related Transportation

Performance-Based Earthquake Engineering Assessment Tool for Gas Storage and Pipeline Systems is the final report for Contract Number PIR-18-003 conducted by Jonathan Bray and Norman Abrahamson of the University of California, Berkeley, and Jennie Watson-Lamprey and Micaela Largent of Slate Geotechnical Consultants, Inc. The information from this project contributes to the Energy Research and Development Division's Gas Research and Development Program.

For more information about the Energy Research and Development Division, please visit the CEC's research website (www.energy.ca.gov/research/) or contact the Energy Research and Development Division at ERDD@energy.ca.gov.

ABSTRACT

Earthquakes impact the safety and reliability of gas storage and transmission systems. Current risk studies performed by utility owners and operators are derived from risk scoring that is highly subjective and qualitative, which do not provide the framework for proper incorporation of uncertainties. The reliability of the risk assessments needs improvement through reducing uncertainties with quantitative data. A new open-source seismic risk assessment tool, *OpenSRA*, was developed to enable system regulators and operators to address challenges posed by the risk from earthquakes and to reliably prioritize the most impactful seismic retrofits for gas infrastructure in California. *OpenSRA* incorporates new methods to assess the seismic risk of gas infrastructure due to multiple geohazards, and it incorporates new seismic capacity ("fragility") curves for gas system components based on highly efficient modeling and laboratory testing supplemented by validation processes for more reliable assessments. *OpenSRA* provides an analysis framework grounded on a methodical performance-based quantitative approach instead of an ad hoc qualitative approach. With *OpenSRA*, assessments are built from robust quantitative data for seismic demand and seismic capacities of gas storage, pipeline systems, and their components.

TABLE OF CONTENTS

LIST OF FIGURES

LIST OF TABLES

Executive Summary

Background

Earthquakes directly impact the safety and reliability of gas storage and transmission systems. Current risk studies performed by gas utilities on their pipelines and storage facilities are subjective and qualitative. One of the main concerns of current risk assessment practices is the uncertainty created by data inaccuracy. To bolster the reliability of these risk assessments, uncertainties must be improved with quantitative data. This project reduces and defines the uncertainties associated with typical risk assessment by defining seismic demand (such as ground shaking or displacement due to an earthquake) models for different levels of data. This project's research also expands the knowledge of the seismic capacity (the ability of a structure to resist and withstand the forces generated by seismic events), or fragility, of gas infrastructure.

System-wide fragilities and prioritizing mitigation will provide greater safety and reliability of the overall system. Mitigation decisions based on robust quantitative data can result in effective disbursement and lower overall costs. Vulnerable system components can be repaired or strengthened before failure, avoiding adverse environmental impacts and supporting public health and energy security.

Project Purpose and Approach

The overall goal of this project was to develop an open-source research-based seismic risk assessment tool (*OpenSRA*) for gas system regulators and operators to better understand and address state-wide risks, prioritize mitigation, plan new gas infrastructure and retrofits, and help focus on post-earthquake repair work.

The project team included researchers from University of California, Berkeley; Lawrence Berkeley National Laboratory; University of California, San Diego; University of Nevada, Reno; the Pacific Earthquake Engineer Research (PEER) Center; the National Hazards Engineering Research Infrastructure SimCenter; and Slate Geotechnical Consultants and its subcontractors Lettis Consultants International and Thomas O'Rourke of Cornell University

The seismic demands that were assessed included ground shaking, fault displacement, liquefaction-induced lateral spreading, liquefaction-induced settlement, and seismic-induced landsliding. The components of the gas infrastructure that were considered included wells and caprocks, aboveground infrastructure, and buried pipelines. The seismic demands and seismic capacities were then implemented into the open-source software *OpenSRA* to help regulators and utility owners calculate the probability of failure occurring in their system.

To monitor successful progress of this project, these performance metrics were established: website clicks, user workshop attendance, lab testing goals, and validation results.

Key Results

The primary result of this project was the development of the *OpenSRA* software, which is available to the public through the PEER Center website. The *OpenSRA* software addresses several of the concerns associated with the informal manner in which current seismic risk assessments of gas pipelines and storage facilities are performed. The *OpenSRA* software implements performance-based earthquake engineering framework through fragility curves that describe the seismic performance of key gas infrastructure components. The developed models embedded in the software allow end users to quantify the seismic risks of buried pipelines, wells and caprocks, well-trees, and pressure vessels. Using the *OpenSRA* software, end users can input data available to a site, a region, or statewide, predict the seismic demand, and compute the probability of failure both visually and tabularly. *OpenSRA* provides flexibility to end users by allowing use of default values recommended by the research team in the case where user-defined inputs are not available.

Improved models of earthquake-induced ground failure hazards (specifically, liquefaction-induced lateral spreading and earthquake shaking-induced landslides) were developed to better capture these hazards at different levels of regional scale analysis. The uncertainty assigned to the ground failure hazard models at different regional scales is consistent with the information available in California at the state-wide, regional, and site-specific levels.

Experiments of pipe components and subsystems provided critical insights into their seismic performance. The experiments identified the early signs and damages that would lead to component or subsystem failures, and the test data was used to develop the frailty curves of these components and subsystems. Advanced analysis of gas storage wells identified key response characteristics on their seismic performance. New sensing technologies were identified and reviewed that can inform the risk models at the input, intermediate, and final output stages. Validation of the models and the software was conducted at four demonstration sites, and the analysis results correlated well with documented observations after specific earthquakes (Bain et al., 2023).

Knowledge Transfer and Next Steps

Project methods and results were shared with multiple users to ensure that *OpenSRA* had the best chance of being adopted by industry. A project website was developed (https://peer.berkeley.edu/opensra) for the public, with a central repository that is continuously updated with the research goals, tasks, findings, and development of *OpenSRA*. Notifications of research findings and their significance to the *OpenSRA* software were issued by PEER electronic newsletters and social media channels (LinkedIn, Twitter, and Facebook).

Presentations about the project, research basis, and applications were made at workshops and conferences targeted to other natural hazards engineering researchers, practitioners, and stakeholders/users. Most notably, the project progress was featured in a special technical session, *Seismic Risk Assessment Methodologies and Open-Source Tools for Natural Gas Infrastructure*, at the 12th National Conference on Earthquake Engineering in 2022. These presentations are summarized on the project website at https://peer.berkeley.edu/opensra/related-news.

During the project development, meetings were held with a technical advisory committee composed of representatives from the California Energy Commission, California Geologic Energy Management Division, California Public Utilities Commission, and user utilities such as Southern California Gas Company (SoCalGas) and Pacific Gas and Electric Company (PG&E). The technical advisory committee helped set the project team's research objectives, provided insights into industry technical needs, and asked probing questions during the meetings. A user workshop was also held to facilitate the use and broader application of the software tool. The user workshop had around 80 registrations globally, with 31 in-person attendees.

Finally, the project team met with PG&E and SoCalGas to provide software tool demonstrations and discuss their needs throughout the project. For instance, the team adopted a utility recommendation to focus on high-pressure transmission lines in high-consequence locations that are more vulnerable to seismic events. The interaction with utilities will better enable potential adoption of the *OpenSRA* software.

Future development of *OpenSRA* would benefit from additional research in the following general areas:

- Pipeline response to additional geometric configurations, or to support variations such as pipelines attached to bridges.

- Extension of the numerical models of soil-pipeline response for additional loading scenarios.

- Optimization of model updates using information from sensing technologies installed on infrastructure systems.

- Integration with United States Geological Survey ShakeMap scenarios, more complex rupture scenarios, or other forms of natural hazards.

- Integration into infrastructure types that have upstream/downstream interdependencies.

- Development of the software backend for computational efficiency as enhancements are added to the software.

- Extension of the software to web-based use for broader access.

The expanded use of *OpenSRA* will continue to be informed by input and feedback from user-driven needs and applications that provide data needed for decision making.

CHAPTER 1:
Introduction

The current state of practice for seismic risk assessment of gas infrastructure includes risk scoring approaches, which are highly subjective and qualitative. These methods either do not estimate/incorporate uncertainties, require the user to estimate them based on outdated data and engineering judgement, or greatly overestimate uncertainties due to lack of data. This can lead to an incorrect estimation of seismic risk and the probability of failure for the system. Additionally, current tools lack transparency, and utility stakeholders often do not know how the risk assessment is being performed. These concerns were addressed through the updated methods, incorporation of uncertainties, and open-source nature of this project and the software created.

The overall goal of the *OpenSRA* project was to create an open-source research-based seismic risk assessment tool for gas infrastructure that can be used by utility stakeholders to better understand state-wide risks, prioritize mitigation, plan new gas infrastructure, and help focus post-earthquake repair work. This was achieved by conducting user-driven research to develop a comprehensive quantitative seismic risk method using probabilistic data to evaluate and manage the seismic risk for gas storage and pipeline systems. To monitor successful progress of this project, the following metric goals were established at the beginning of the project: website clicks, user workshop attendance, lab testing goals, and validation results. These metrics were associated with project exposure, interest in and use of the software, and improvement of calculation methods.

The probabilistic seismic risk tool developed in this project follows the widely accepted risk method of Cornell (1968). A seismic source characterization is used to develop a suite of earthquake scenarios with associated rates of occurrence to represent the seismic hazard. Fault ruptures and the resulting ground shaking are generated for each earthquake scenario to represent the seismic loading, which includes a map of ground motion parameters. This scenario-based seismic parameter map is overlaid on the infrastructure system, and the seismic loading is related to the capacities of the infrastructure to calculate the seismic performance of the gas system for the scenario. By repeating the process for all the scenarios in the suite, the tool can evaluate the seismic risk to the system.

OpenSRA was developed to be applied easily by regulators and utility owners, and to include updated models and methods for the seismic demands and capacities that control the seismic risk for gas systems; this was done by including the users (utility owners and operators) from the onset. The project included several innovative approaches that improved the basic methodology and distinguished this project's approach from standard approaches currently used. Current risk studies developed by the utilities use risk scoring approaches that are highly subjective and qualitative. They do not properly incorporate the uncertainties in the seismic demand and in the fragility of the system and its components. Targeted research, including liquefaction, landsliding, fault displacement, and fragility of different components of infrastructure, was conducted in this project to improve the characterization of uncertainty of key

inputs to the seismic risk assessment tool. The method used in this project provided quantitative estimates of the probabilistic seismic risk.

This report summarizes the activities and accomplishments of the *OpenSRA* project. It provides a high-level outline of the project components, framework of the *OpenSRA* software, and the resulting fragility curves. Three gas systems were considered in this study: a) buried pipelines, b) underground storage facilities, and c) aboveground storage and transmission systems. The hazards of surface fault rupture, earthquake ground shaking, liquefaction-induced ground movements, and earthquake-induced landslides were characterized in this study. Three levels of analysis may be performed, depending on the quantity and quality of data available and the sophistication of the model that can be used for each data level. Each component of the system has undergone finite element modeling to estimate the response of the component to the ground shaking and ground deformation resulting from each hazard and the resulting probability of failure. The seismic hazard assessments and the finite element modeling results developed as part of this study were used to develop fragility curves that were implemented into *OpenSRA* to aid end users in estimating failures in their systems as well as prioritizing risk mitigation efforts.

CHAPTER 2:
Project Approach

Background

The culminating product of this multi-year project is the *OpenSRA* software. This software is comprised of seismic demand and seismic capacity ("fragility") analyses. Multiple research efforts were undertaken to address these two analysis types, as well as studying the different subsystems and components of gas infrastructure. The *OpenSRA* framework serves as a roadmap for the different elements making up the software. This section describes the framework of *OpenSRA*, the demand analyses performed to reach the final results, and the approach used to calculate fragilities and validate the program. It should be noted that this report provides an overview of a large and multi-disciplinary project. As such, many of the sections reference the California Energy Commission (CEC) reports completed earlier in the project. For more specific information about each of the following sections, please refer to these previous reports.

Multiple organizations contributed to this project to perform all the necessary components. The project team included researchers from University of California, Berkeley; Lawrence Berkeley National Laboratory; University of California, San Diego; University of Nevada, Reno (UNR); the Pacific Earthquake Engineer Research (PEER) Center; the National Hazards Engineering Research Infrastructure SimCenter; and Slate Geotechnical Consultants and its subcontractors Lettis Consultants International and Thomas O'Rourke of Cornell University.

Focused research to advance the seismic risk assessment tool was conducted by task groups, each addressing a particular area of study and expertise and collaborating with the other groups. The tasks were as follows:

> Task A: Fault displacement
> Task B: Liquefaction-induced deformation and seismically induced slope displacement
> Task C: Performance of gas storage well casings and caprock
> Task D: Performance of gas storage and pipeline system surface infrastructure
> Task E: Smart gas infrastructure sensing of wells and pipeline connections performance
> Task F: Synthesis of component fragilities into a system performance model

Targeted research was conducted in this project to improve the characterization of the uncertainty of key inputs. The uncertainties were further defined with levels of analysis. Three levels of analysis may be performed, depending on the quantity and quality of data available and the sophistication of the model that can be used for each data level. Level 1 is a statewide analysis, Level 2 is a regional analysis, and Level 3 is a site-specific analysis. Each component of the system has undergone finite element modeling to estimate the response of the component to the ground shaking and ground deformation resulting from each hazard and the resulting probability of failure.

OpenSRA

OpenSRA is an open-source seismic risk assessment tool developed to assess the seismic risk of gas infrastructure. The software implements the six task groups outlined above to calculate the seismic demand, damage, and risk of failure for gas systems. The following sections outline the framework and calculation components and highlight the new-to-industry calculation methods utilized within *OpenSRA*.

Framework

OpenSRA follows performance-based earthquake engineering (PBEE) risk methodology developed by PEER (Moehle and Deierlein, 2004) to assess the seismic risk of gas infrastructure. The PBEE risk methodology uses a combination of probabilities to calculate the risk of a "decision variable" occurring. These calculations can be lengthy, as there are multiple probability density functions to not only calculate but also integrate over to develop estimates and their uncertainty. To perform the calculations within *OpenSRA* in a timeframe that is useful to the user, polynomial chaos (PC) was implemented. This methodology requires clearly defined means, aleatory variabilities, and epistemic uncertainties for each step of the PBEE risk methodology. For more detailed information regarding *OpenSRA* and PC, please refer to Zheng et al. (2023).

Efficient Evaluation of the PBEE Risk Framework

The risk framework is simply presented as a triple integral (Equation 1) adapted from Moehle and Deierlein (2004).

Equation 1

$$\lambda_{dv} = \int_{DM} \int_{EDP} \int_{IM} P\{DV > dv|dm\} \, p\{dm|edp\} \, p\{edp|im\} \, \lambda_{im} d(im)d(edp)d(dm) \qquad (1)$$

In this equation, IM is the intensity measure (such as peak ground acceleration), EDP is the engineering demand parameter (for example, ground deformation), DM is the damage measure (such as pipe strain), DV is the decision variable (for example, rate of rupture), λ is the annual rate, and the operations of $p\{y|x\}$ and $P\{Y > y|x\}$ are the conditional probability density function and the cumulative distribution function, respectively, of y given x. Given these definitions, λ_{IM} is the annual rate of occurrence of the seismic event, $p\{edp|im\}$ is the probability of a system response computed using geohazard models given the seismic demand, $p\{dm|edp\}$ is the fragility assessment given the system response, and $p\{dv|dm\}$ is the loss estimate given the damage level.

The method presented by Lacour and Abrahamson (2021) approximates probability density functions and cumulative distribution functions as linear combinations of set basis functions (analogous to the Taylor expansion of analytical functions), which are then incorporated into the analytical solution mentioned previously. The primary computation required for PC is the intermediate calculation of the PC terms, which are functions of the various σ_Y and σ_{μ_Y} for IM, EDP, DM, DV, and the linear approximation coefficients for EDP, DM, DV. This set of

intermediate calculations is very fast and efficient to perform, because the PC terms are evaluated analytically. Furthermore, the polynomial functions are known mathematical functions, and the sampling of the uncertainty is performed only once during post-processing, after the PC terms have been fully computed for all events. Overall, as discussed in Lacour and Abrahamson (2021), the use of PC over traditional Monte-Carlo sampling can easily improve the computation time by two to three orders of magnitude. For additional details on the application of PC to the risk framework and validation examples, please refer to Lacour and Abrahamson (2023).

OpenSRA **Overview**

Given the PBEE framework, each of the research tasks split their approaches to fulfill each of the probabilities. Figures 1, 2, and 3 show the workflow of *OpenSRA* and how the PEER risk methodology shown in Equation (1) was conceptually incorporated into the seismic risk assessment of each of the three infrastructure types: below-ground pipelines, wells and cap-rocks, and aboveground subsystem components (Tasks B, C, and D, respectively). The PEER risk method served as the backbone of the *OpenSRA* risk assessment workflow. The user defines the infrastructure type that will be analyzed by *OpenSRA* and inputs the component characteristics. *OpenSRA* then works through the PEER risk method, as shown in the flow charts in these figures, to perform the risk assessment.

As shown in Figure 1, the workflow for below-ground pipelines captures the influence of seismic intensity on ground deformation, the influence of ground deformation on pipe strain, and, finally, the influence of pipe strain on the probability of failure in the form of failure and leakage. The models to relate seismic intensity to ground deformation are based on state-of-the-art models that have been published in literature (Bain et al., 2022). The models to relate deformation to pipe strain and pipe strain to failure are developed as part of the focus of Task B and Task F. These models are described in detail in the following sections.

Figure 1: PEER Risk Method Applied to Below-ground Pipelines

Source: Zheng et al. (2023)

8
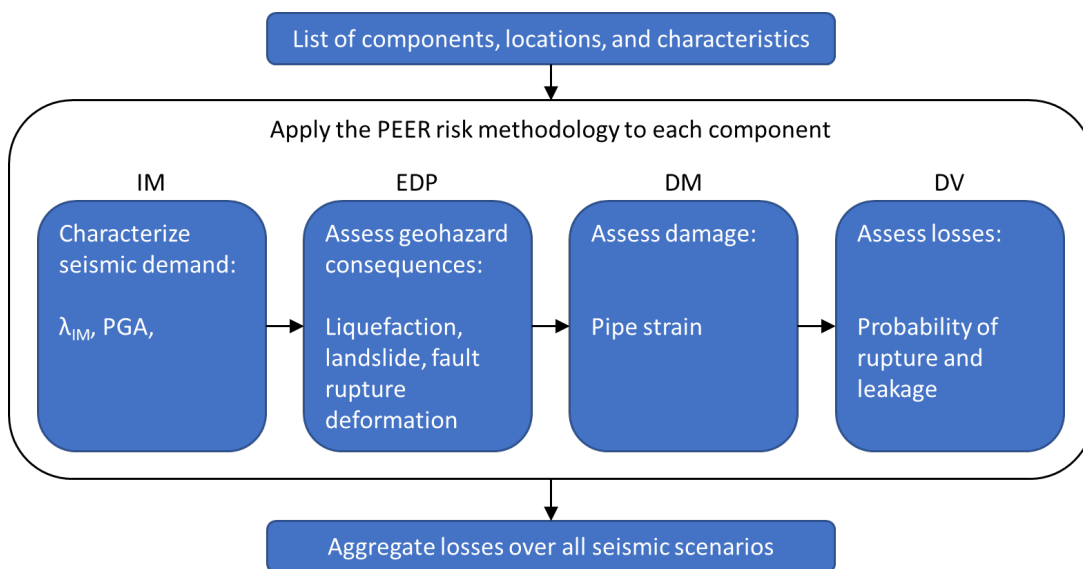
Figure 2 shows the workflow for wells and caprocks. For this category, Task Groups C and F developed damage models for well casings and tubings that are dependent on fault rupture deformation and ground shaking. These models are considered two independent modes of failure for wells. For caprocks, results of the numerical study suggest that the probability of leakage is not significantly dependent on the tested model parameters; hence its distribution is independent of seismic and geohazard demands, and the overall risk is a constant distribution.

Figure 2: PEER Risk Method Applied to Wells and Caprock
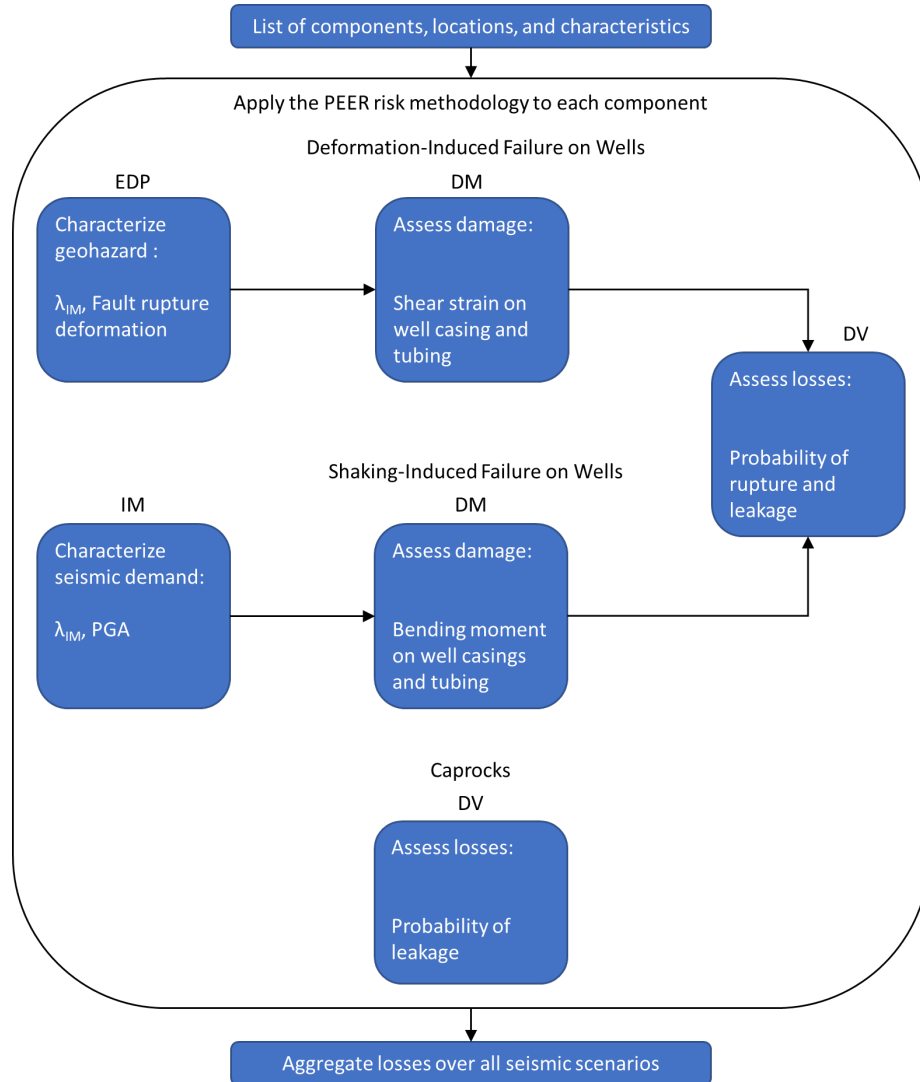
Source: Zheng et al. (2023)

Figure 3 shows the workflow for aboveground subsystem components, specifically the failure associated with wellheads and pressure vessels. Research by Task Groups D and F resulted in models for joint rotations and strains for wellheads and moment ratios for pressure vessels, both of which are dependent on seismic intensity (peak ground acceleration). The intensity of the strains and moment ratios were then used to inform the levels of failure associated with wellheads and pressure vessels, respectively.

Figure 3: PEER Risk Method Applied to Aboveground Components
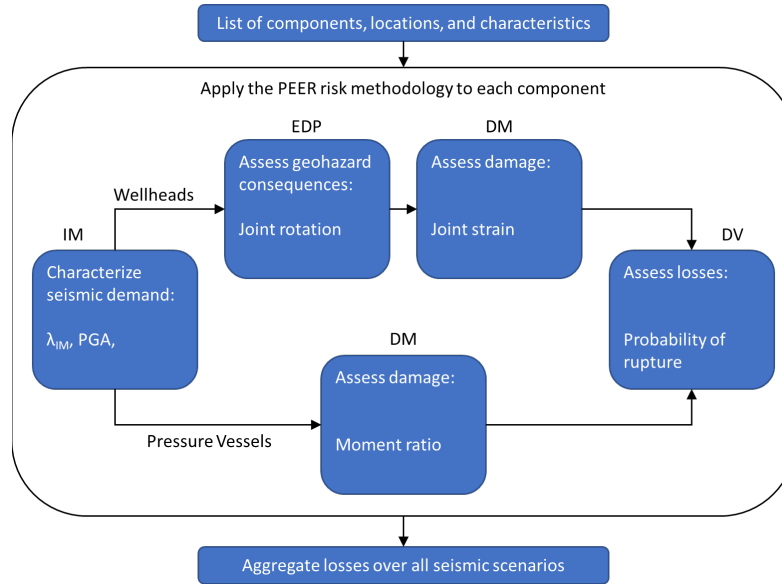
Source: Zheng et al. (2023)

Figure 4 shows a flow chart of the overall user process for *OpenSRA* and how the PEER risk framework is wrapped into the user experience. The user starts with entering general information and with selecting if the default values should be used for the analysis. Once these items, and more specific information (if not using the default values), are entered, the user can run the analysis and visualize the results.

Figure 4: *OpenSRA* User Experience Flow Chart
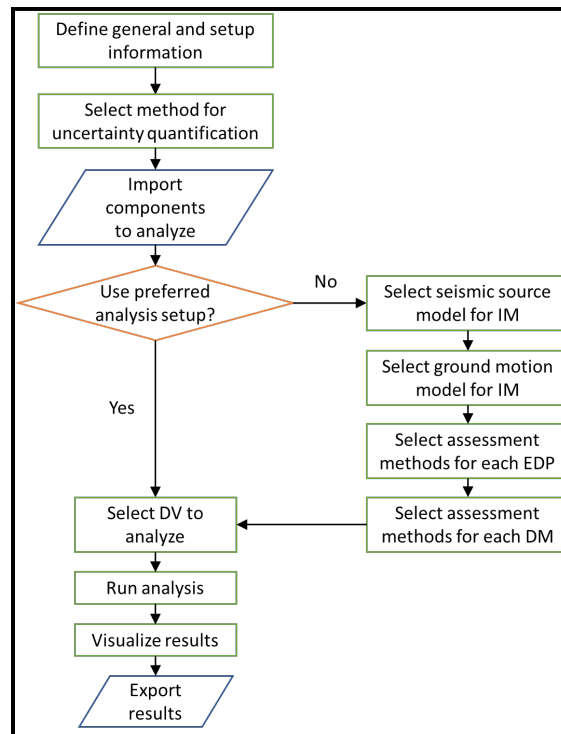
Source: Zheng et al. (2023)

Seismic Hazard Characterization

The ground shaking at a site is estimated by performing a probabilistic seismic hazard analysis (PSHA) using a combination of UCERF3.1 (third Uniform California Earthquake Rupture Forecast) scenarios and ground motion models presented in the Next Generation Attenuation Relationships for Western US (NGA-West2) Project. The PSHA is performed in a preprocessing step that follows the approach first developed by Cornell (1968), with the inclusion of parameters for randomization and the consideration of epistemic uncertainty.

The seismic hazard (and therefore estimated ground motion) is calculated within *OpenSRA*. Similar to the fault displacement hazard (described in the next section), the rupture scenarios are determined using UCERF3.1. Running the entire list of rupture scenarios within *OpenSRA* would require a long computing time, as it is comprised of 253,394 rupture scenarios. For the purposes of this hazard, the UCERF3.1 scenarios were reduced to 1194 scenarios with a magnitude step size 0.5. Additional information about the reduced list of rupture scenarios can be found in Lacour and Abrahamson (2023).

The ground motion is characterized by using a suite of four ground motion models from NGA-West2. Ground motions can also be estimated directly by using ShakeMaps online (Wald et al., 2005). *OpenSRA* calculates the closest point of ground shaking (from ShakeMaps) to wherever the analysis bounds are located. Finally, users can also perform a deterministic scenario by defining a simple fault and using the same weighted NGA-West2 models.

Fault Displacement Hazard

A report titled *Fault Displacement Hazard Characterization for OpenSRA* by Thompson (2021) was previously submitted to the CEC. Please refer to this report for additional details on the model. The primary goal of this subtask was to research models to estimate primary and secondary fault displacement hazard, and where this fault displacement hazard impacts underground pipelines, wells, and caprocks.

Throughout this report, the seismic demands outlined are split into levels. These levels correlate to the scale at which the analysis is performed and the quantity of data available. Level 1 is a statewide analysis, Level 2 is a regional analysis, and Level 3 is a site-specific analysis. Guidance for implementing the fault displacement hazard element to *OpenSRA* for the various levels is captured in the hazard matrix table in Thompson (2021). The recommended models, inputs, and outputs are presented in Table 1.

Table 1: Fault Displacement Models Implemented Into *OpenSRA*

Level	Model	Inputs	Outputs
Level 1	Wells and Coppersmith (1994)	UCERF3-linked Q-fault scenarios, including magnitude, dip, strike, rake	Fault displacement magnitude and direction
Level 2	Petersen et al. (2011)	UCERF3-linked Q-fault scenarios, including magnitude, dip, strike, rake	Fault displacement magnitude and direction

Level	Model	Inputs	Outputs
Level 3	PFDHA models (not yet publicly available)	Beyond the scope of this project	Fault displacement magnitude and direction

Source: Zheng et al. (2023)

The fault-pipeline crossing algorithm for Levels 1 and 2 uses Q-faults (USGS and CGS, 2006) to map fault location while continuing to utilize UCERF3.1 for the rupture geometry (strike, dip, rake) and magnitude. A 100-meter buffer around the Q-fault traces defines the fault polygon, and the nearest UCERF3 fault defines the rupture attributes. Figure 5 depicts the Q-fault locations, along with pipeline crossings (shown with stars). Figure 6 shows the primary and secondary fault zones developed by Thompson (2021). The pipeline shapefile is divided into straight, 100-meter segments to track the specific segments that cross fault zones. These mapped faults, along with their calculated displacement vectors (described further in Zheng et al., 2023), are then used in the fragility development of buried pipelines, wells, and caprocks.

Figure 5: Intersections of Gas Pipelines in California with Fault Traces From the U.S. Quaternary Fault and Fold Database (2019 edition)
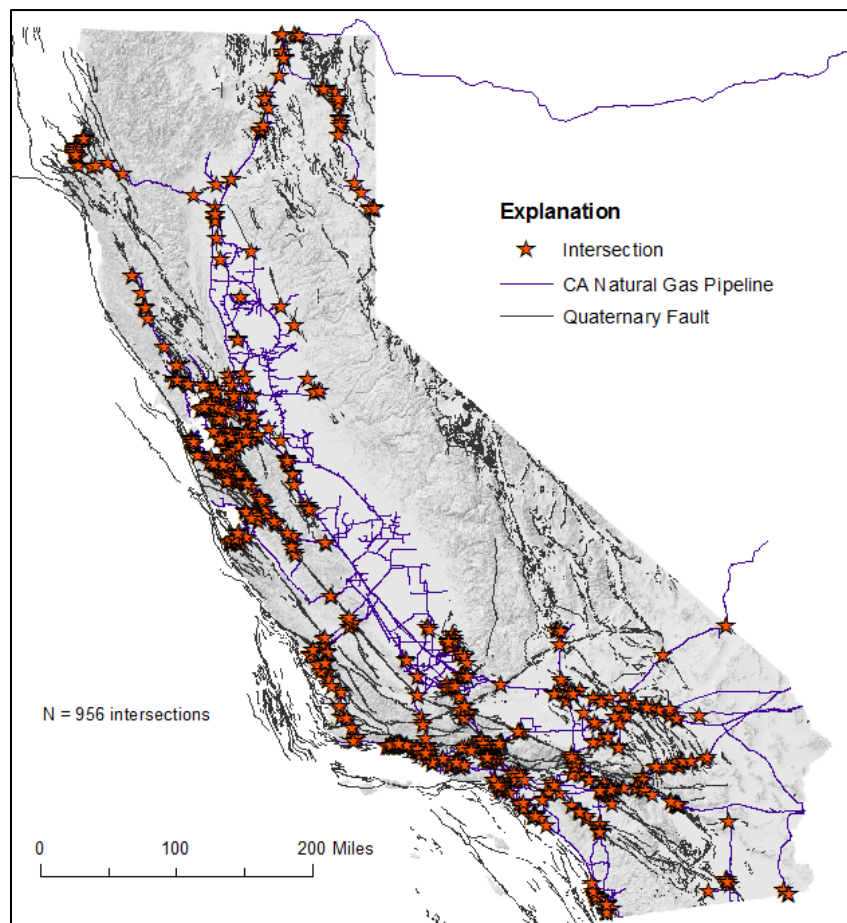
Map of California showing gas pipelines (in blue) and fault traces from the U.S. Quaternary Fault and Fold Database (in gray). The 956 intersections of these two linear datasets are indicated by red stars.

Source: Pipeline database from the CEC. Fault source traces from USGS and CGS (2006).

Figure 6: Level 2 Primary and Secondary Fault Hazard Zones and California Pipelines in the San Francisco Bay Area
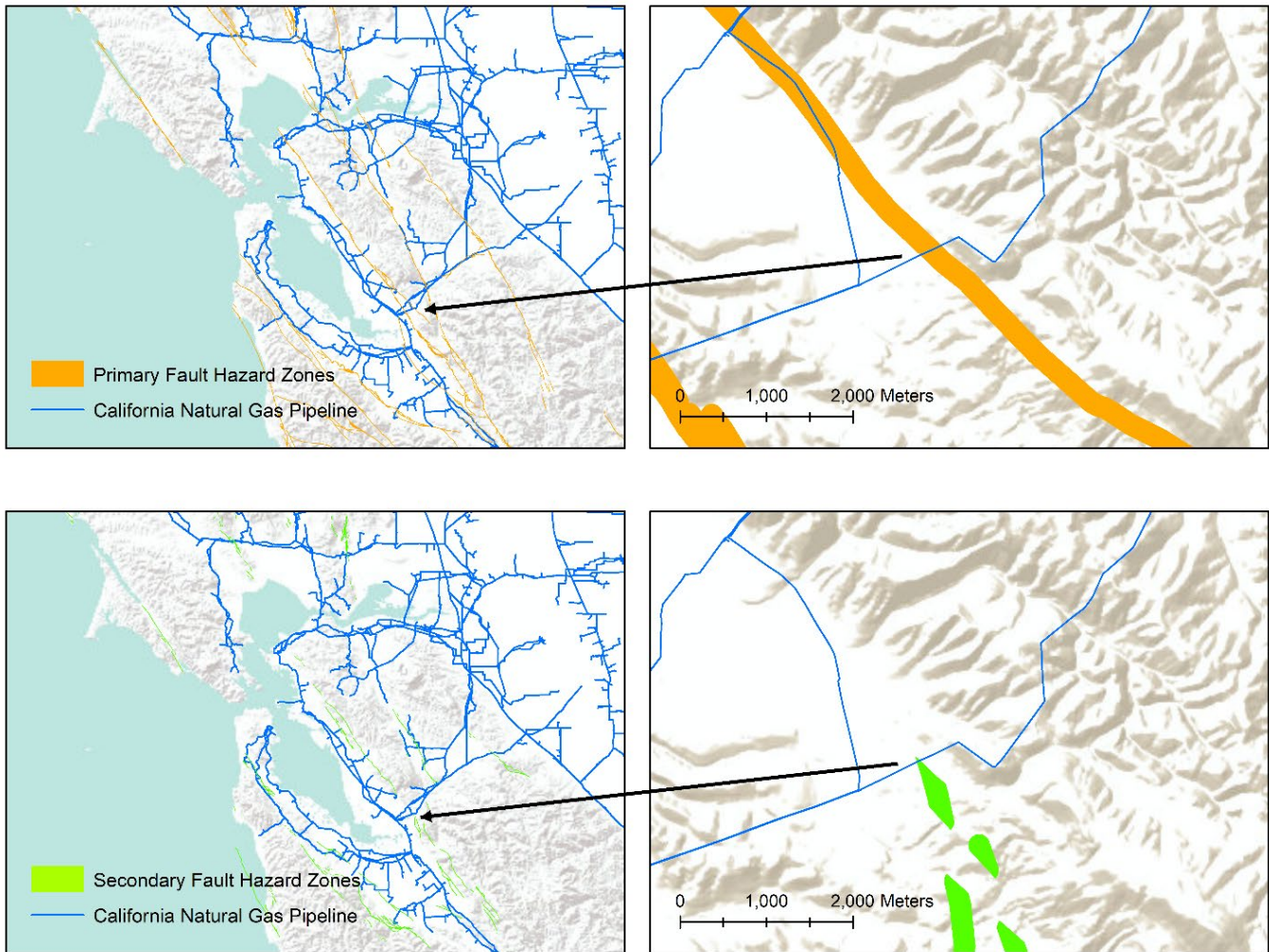
The left-side figures show primary (orange) and secondary (green) fault hazard zones. The right side figures show examples of pipeline-fault zone intersections.

Source: Pipeline database from the CEC. Fault source zones developed by Thompson (2021).

Liquefaction and Landsliding

A report titled *Enhanced Liquefaction and Ground Deformation Report* by Bain et al. (2022) was previously submitted to the CEC. Please refer to this report for additional details on these models. This task group explored different earthquake-induced geohazards, such as liquefaction, lateral spreading, and landsliding. Similar to Fault Displacement Hazard, these demands were split into different levels of analysis. The task group focused on estimating the EDP and DM for buried pipelines. The following sections outline the different EDPs considered (within this task group). The results of the damage model to predict strain are presented in the "Results" section.

Liquefaction Triggering Models and Data

The models implemented into *OpenSRA* to calculate the probability of liquefaction are outlined in Table 2.

Table 2: Models for Liquefaction Triggering

Level	Model	Inputs	Model
Level 1	Zhu et al. (2017)	PGV, Vs30, precipitation, D_c, D_r, D_w, GWT	Probability of liquefaction
Level 2	Youd and Perkins (1978) with Hazus (FEMA, 2020)	Surficial quaternary geologic maps, PGA, M_w, GWT	Liquefaction susceptibility converted to probability of liquefaction
	Bain and Bray model (undergoing publication peer review)	Surficial quaternary geologic maps, PGA, M_w, GWT	Probabilistic assessment of liquefaction triggering and lateral spread displacement
Level 3	Boulanger and Idriss (2016)	CPT, PGA, M_w, GWT	Probability of liquefaction
	Probabilistic Modification to Robertson and Wride (1998) updated as Robertson (2009) from Ku et al. (2012)	CPT, PGA, M_w, GWT	Probability of liquefaction
	Moss et al. (2006)	CPT, PGA, M_w, GWT	Probability of liquefaction

Source: Zheng et al. (2023).

Liquefaction-induced Lateral Spread Displacement and Vertical Settlement Models and Data

Table 3 outlines the models for the probability of liquefaction-induced settlement. Table 4 outlines the models for lateral spreading. For lateral spreading specifically, an updated Level 2 analysis is proposed to enable the use of enhanced data (when compared to Level 1). This method is briefly outlined; more information can be found in Bain et al. (2022).

At Level 2, the Hazus (FEMA, 2020) method can be applied to estimate potential lateral spread displacement and vertical settlement due to liquefaction. However, because enhanced data are available at Level 2 compared to Level 1, research has been performed to develop a new Level 2 procedure for assessing lateral spread displacement.

The proposed procedure is based on liquefaction probability curves for surficial geologic units, described in Holzer et al. (2011). This research has modified and expanded the framework of the Holzer et al. (2011) procedure to include assessments for the probability of liquefaction triggering, potential lateral spread displacements, and estimates of their uncertainties. For further information on the development of this procedure, please see Bain et al. (2022). An example of these expanded and updated curves is shown in Figure 7 and Figure 8, where LDI is the lateral displacement index.

Table 3: Liquefaction-induced Settlement Models Implemented Into *OpenSRA*

Level	Model	Inputs	Model
Level 1	Zhu et al. (2017) combined with Hazus (FEMA, 2020)	PGV, V_{s30}, precipitation, D_c, D_r, D_w, GWT	Liquefaction susceptibility class converted to settlement estimate
Level 2	Zhu et al. (2017) with Hazus (FEMA, 2020)	PGV, V_{s30}, precipitation, D_c, D_r, D_w, GWT	Liquefaction susceptibility class converted to settlement estimate
	Youd and Perkins (1978) with Hazus (FEMA, 2020)	Surficial quaternary geologic maps, PGA, M_w, GWT	Liquefaction-induced settlement according to liquefaction susceptibility category
Level 3	Cetin et al. (2009)	SPT, GPA, Mw, GWT	Free-field, level-ground settlement
	Zhang et al. (2002)	CPT, PGA, Mw, GWT	Free-field, level-ground settlement

Source: Zheng et al. (2023).

Table 4: Lateral Spread Models Implemented Into *OpenSRA*

Level	Model	Inputs	Outputs
Level 1	Zhu et al. (2017) with Hazus (FEMA, 2020)	PGV, V_{s30}, precipitation, D_c, D_r, D_w, GWT	Liquefaction susceptibility class converted to settlement estimate
Level 2	Youd and Perkins (1978) with Hazus (FEMA, 2020)	Surficial quaternary geologic maps, PGA, M_w, GWT	Liquefaction susceptibility converted to lateral spread displacement
	Proposed model presented in Bain et al. (2022)	Surficial quaternary geologic maps, PGA, M_w, GWT	Probabilistic assessment of liquefaction triggering and lateral spread displacement
Level 3	Zhang et al. (2004)	CPT, PGA, M_w, GWT, topographic slope or free-face ratio	Estimate of lateral spread displacement
	Idriss and Boulanger (2008) combined with Zhang et al. (2004)	CPT or SPT	Estimate of lateral spreading displacement

Source: Zheng et al. (2023).

Figure 7: Prob(LDI="0") Versus PGA/MSF Data for Afem Deposits
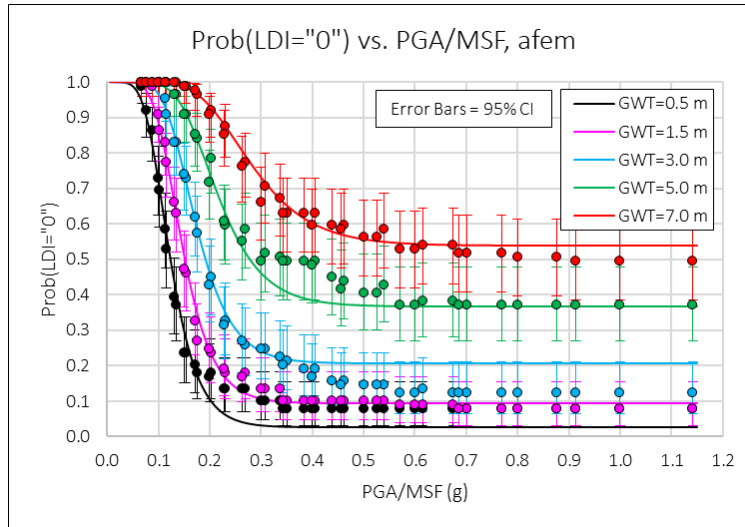
Fit of Prob(LDI="0") regression model to data calculated for sandy artificial fill over Bay Mud deposits

Source: Bain et al. (2022)

Figure 8: Mean, Non-zero LN(LDI) Data for Afem Deposits
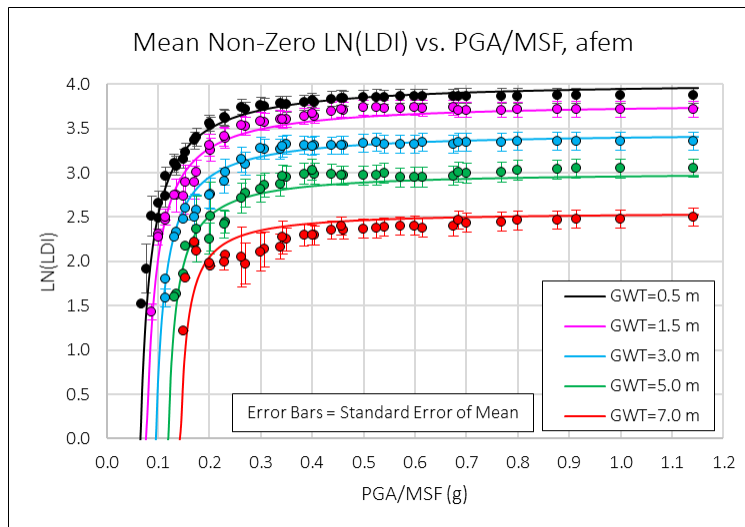
Fit of mean, non-zero LN(LDI) regression model to data calculated for sandy artificial fill over Bay Mud deposits

Source: Bain et al. (2022)

The Prob(LDI="0") and non-zero LN(LDI) data are combined using a mixed random variable model, as illustrated in Figure 9. These models estimate only a distribution of LDI. The estimated LDI distribution is converted to a distribution of lateral spread displacement using topographic correlations of LDI to lateral spread displacement (Zhang et al., 2004). Although this method has been shown to provide reasonable results in the San Francisco Bay Area and in Christchurch, New Zealand, it requires sufficient cone penetration test (CPT) data over an area to implement it in *OpenSRA*. At present this new procedure is implemented in *OpenSRA* only in the San Francisco Bay area.

16

Figure 9: Comparison of Continuous and Mixed Random Distributions
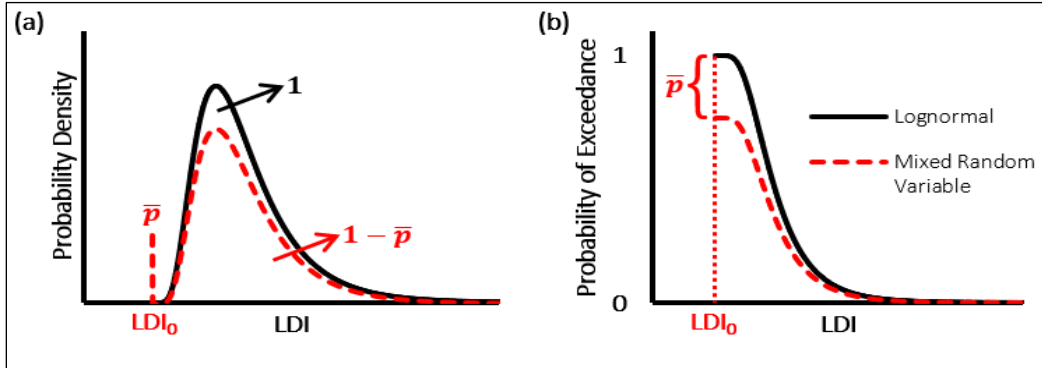
(a) Probability density function for a mixed and continuous random variable, and (b) probability of exceedance for a mixed and continuous random variable

Source: Bain et al. (2022)

Seismic Slope Stability and Slope Displacement Models and Data

Table 5 outlines the proposed seismic-induced landsliding models that have been implemented into *OpenSRA*.

Table 5: Seismic-induced Landslide Models Implemented Into *OpenSRA*

| Level	Model	Inputs	Outputs
Level 1	Infinite slope analysis using strength distributions presented in Table B.15 in Bain et al. (2022)	Statewide Geologic Map	Estimate of seismic slope displacement
Level 2	Grant et al. (2016)	Topographic slope, ϕ, γ, c, c_r, t, PGA	Model predicts the type of slope movement (rock-slope failures, disrupted soil slides, coherent rotational slides, and lateral spreads) and estimates the seismic slope displacement distribution
	Bray and Macedo (2019)	Topographic slope, ϕ, γ, c, t, PGA, M_w	Seismic slope displacement distribution
Level 3	Zhang et al. (2004)	CPT, PGA, M_w, GWT, topographic slope or free-face ratio	Estimate of lateral spread displacement
	Idriss and Boulanger (2008) combined with Zhang et al. (2004)	CPT or SPT	Estimate of lateral spread displacement

Source: Zheng et al. 2023

Fragility Curve Development

Each research task was responsible for developing fragility curves for a specific component of gas infrastructure. This is represented in the PBEE framework in the "DM" and "DV" probabilities. More information can be found in (Watson-Lamprey et al., 2022).

Each research task performed sensitivity studies to find the input parameters that changed the probability of failure the most. It then defined the necessary inputs for the model, assigned ranges based on manufacturer guidance or expert opinion (mean and standard deviation), and, finally, changed each input individually (within its range) to see which parameters impacted the final answer. From there, the teams estimated damage models (probability of a strain level, given an intensity measure) and fragility models (probability of failure, given a strain or deformation), using a variety of laboratory testing and finite element modeling. These fragility curves were implemented into *OpenSRA* within each component calculation (underground pipelines, wells and caprocks, and surficial infrastructure). Further information on individual fragility curves is presented in the "Results" section of this report.

OpenSRA Validation and Use

Validation of *OpenSRA* was one of the key milestones of this project, and a crucial step in the technology transfer. Four sites were chosen to encapsulate the different geohazards, the type of gas infrastructure at the site, and the utility owners' ability to give information to the team. These sites included Balboa Boulevard (a gas pipeline rupture occurred in the 1994 Northridge earthquake but there was no damage in the 1971 San Fernando earthquake), Cordelia Junction (which has a known landslide, based on confidential information shared by PG&E), McDonald Island (which has complex aboveground infrastructure, based on confidential information shared by PG&E), and Honor Rancho (which is close to many faults and has a large well field and caprock). The results from *OpenSRA* showed that the probabilities of subsystem leakages and ruptures were consistent with both observations at the sites and expected performance of these subsystems. In particular, the Level 3 analysis at the Balboa Boulevard site generated results similar to what actually occurred during the 1994 Northridge earthquake.

Each research team implemented its seismic demand and fragility models into *OpenSRA* and then performed analyses for past earthquakes or test earthquake scenarios to validate the program. More information on this can be found in Bain et al. (2023).

CHAPTER 3:
Results

Introduction

This section outlines the results from the fragility curve development for the different subsystems.[1] This section also includes information on the *OpenSRA* graphical user interface, where the demand and fragility research are synthesized. Finally, project metrics are summarized.

Below-Ground Pipelines

Referring to the *OpenSRA* framework, the previous section outlined the methods to estimate the EDP and, given that EDP, this section focuses on how to estimate the DM. To do this, a numerical model of the soil-pipeline interaction and pipe response to permanent ground deformation was made using Abaqus Version 6.1. Details of the selected scenarios and numerical modeling techniques (such as finite element mesh, beam element type, springs, boundary conditions, integration points) are provided in the Hutabarat et al. (2023) report.

The numerical modeling in this study analyzed only abrupt ("knife-edge") ground movements. These result in locally higher strain concentrations compared to distributed ground movements, which were not studied.

Figure 10 summarizes the ground deformation modes assessed for the *OpenSRA* Project. The following deformations were assessed:

- Pipelines that cross landslides or lateral spreads parallel to the direction of displacement

    - Normal-slip (Figure 10c) at the scarp
    - Reverse-slip (Figure 10d) at the toe
    - The fifth case of ground deformation where no bending strains are induced (similar to Figure 10e)

- Pipelines that cross landslides or lateral spreads perpendicular or at an oblique angle

    - Strike-slip tension (Figure 10a)
    - Strike-slip compression (Figure 10b)

- Ground settlement can be modeled as vertical normal-slip deformation (Figure 10c).

The complete results of the buried gas pipeline system modeling are provided in Hutabarat et al. (2023). Select plots of longitudinal pipe strain versus permanent ground deformation are displayed in Figure 11.

---

[1] See the previously submitted interim project reports for further information regarding specific models and results.

Figure 10: Assessed Ground Deformation Modes
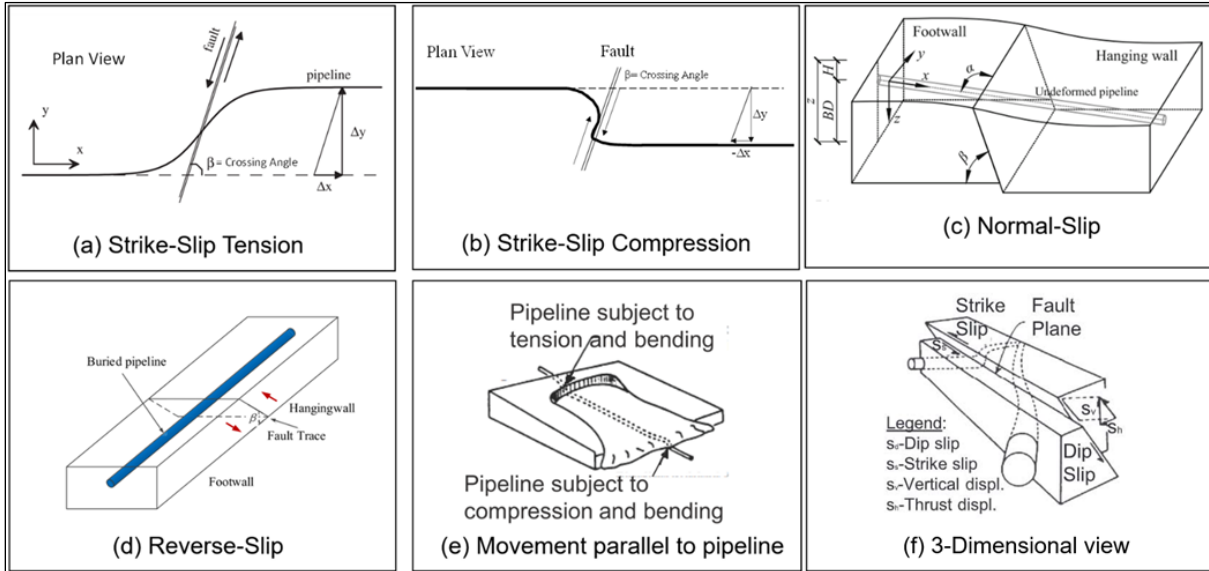
Ground deformation modes assessed to derive pipe strain fragility models.

Source: Bain et al. (2022)

Figure 11: Longitudinal Pipe Strain Versus Ground Deformation Simulation Results
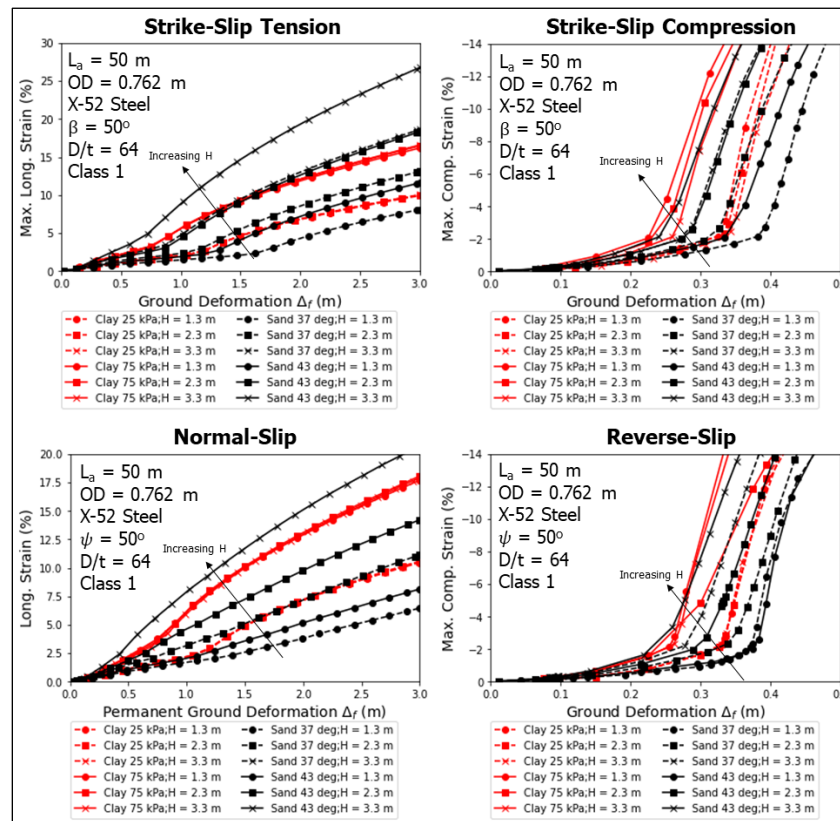
Longitudinal pipe strain versus ground deformation simulation results for soil-pipeline systems subjected to strike-slip tension, strike-slip compression, normal-slip, and reverse-slip ground deformation.

Source: Bain et al. (2022)

Using the parameters found to most affect the results, more than one million numerical simulations of pipelines subjected to permanent ground deformation were performed. The simulation results were used to develop relationships that estimated a distribution of longitudinal pipe strain as a function of the soil-pipeline system parameters.

Figure 12 presents numerical results in terms of the longitudinal strain for representative tensile and compressive failure mode cases. The complete suite of pipe strain estimation models for all cases is provided in Watson-Lamprey et al. (2022).

Figure 12: Modeled Pipeline Response to Tensile and Compressive Pipe Strain
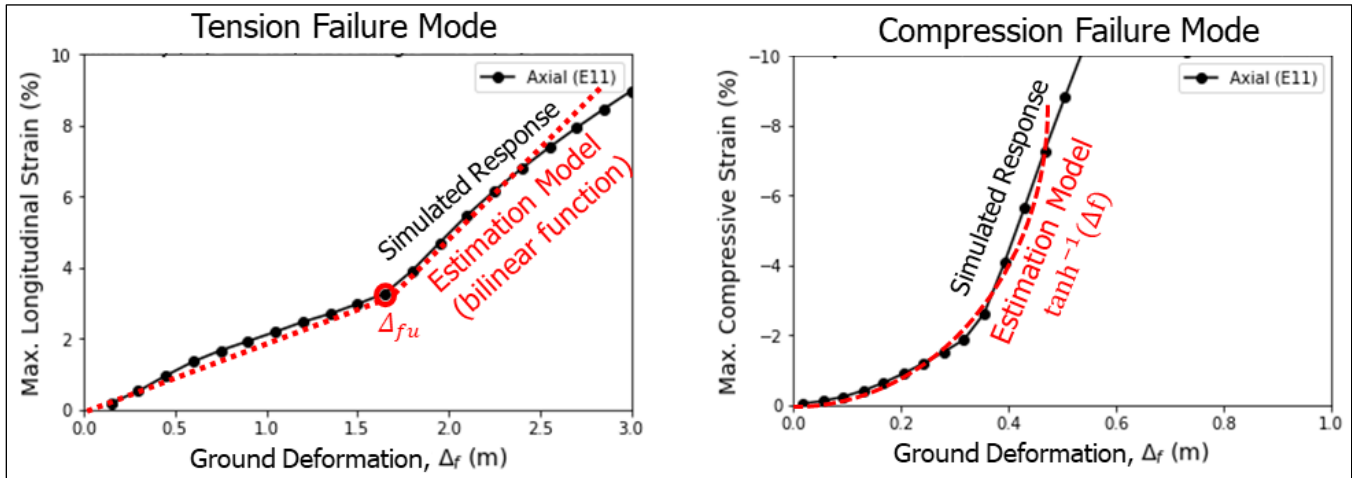
Modeled pipeline response to tensile pipe strain (strike-slip tension or normal-slip mode) and compressive pipe strain (strike-slip compression or reverse-slip mode), with examples of bi-linear and inverse hyperbolic tangent regression models used to capture the simulated responses.

Source: Bain et al. (2022)

Wells and Caprocks

Figure 2 shows the steps within *OpenSRA* to calculate the probability of failure in wells and caprocks. This subtask calculated the DM by estimating a damage and fragility model for wells and caprocks.

Fault Shear Across Wells

This subtask assessed the range of fault displacements that could result in well failure. To achieve this objective, a numerical model, using FLAC3D, was constructed to simulate the behavior of a well during fault displacement. The well comprised the structural elements of the well and the subsurface formation that surrounded it. Figure 13 shows the geometry and boundary conditions of the well shear model.

Figure 13: The Numerical Model for the Well Shear Simulation

(a)   (b)
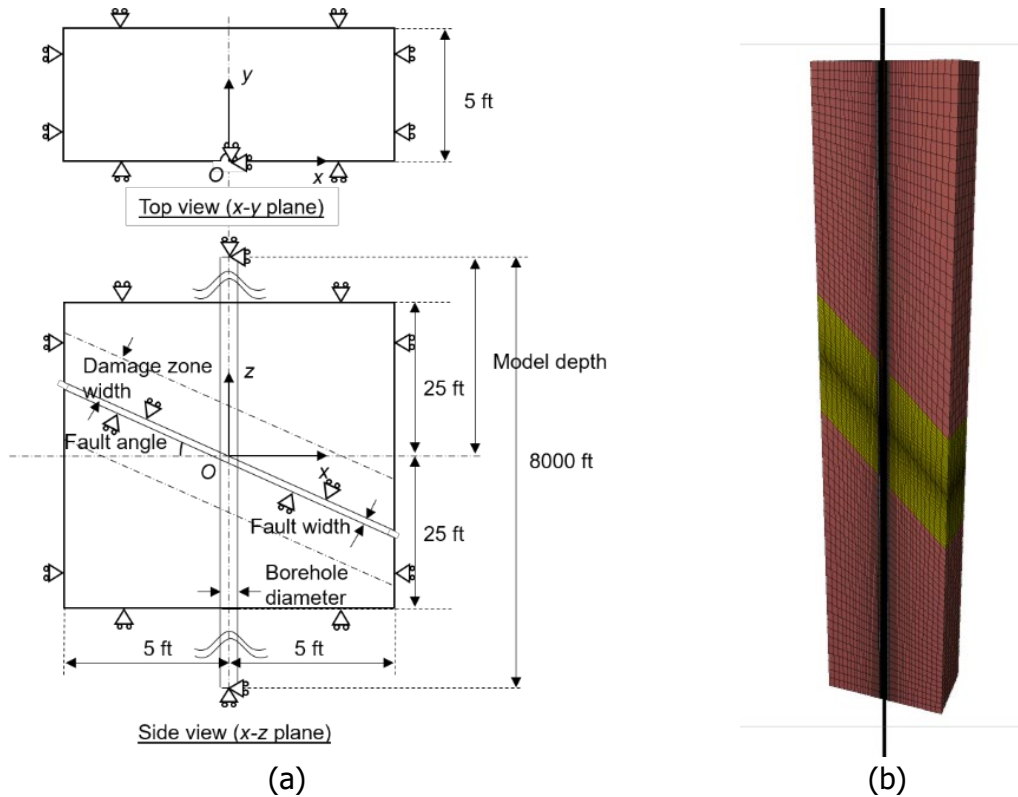
(a) The geometry and boundary conditions of the well shear model, and (b) an overview of the model in FLAC3D (brown is intact rock, dark yellow is the fault zone)

Source: Sasaki et al. (2023)

To include the uncertainty in the depth to the top of cement, two cement scenarios were considered for each well mode, cemented and uncemented annuli. In the former case, the gap between the borehole and the casing was filled with cement, whereas, in the latter case, the gap was left unfilled. Finally, the well shearing process was simulated by modeling reverse fault displacement, as shown in Figure 14. For further information on the materials and models used for this analysis, please see Rutqvist et al. (2022). This numerical model led to both a sensitivity analysis and a well fragility model; more information on this can be found in the section regarding Task Group F as well as in Watson-Lamprey et al. (2022).

Figure 14: Boundary Displacements and Well Shear

(a)   (b)
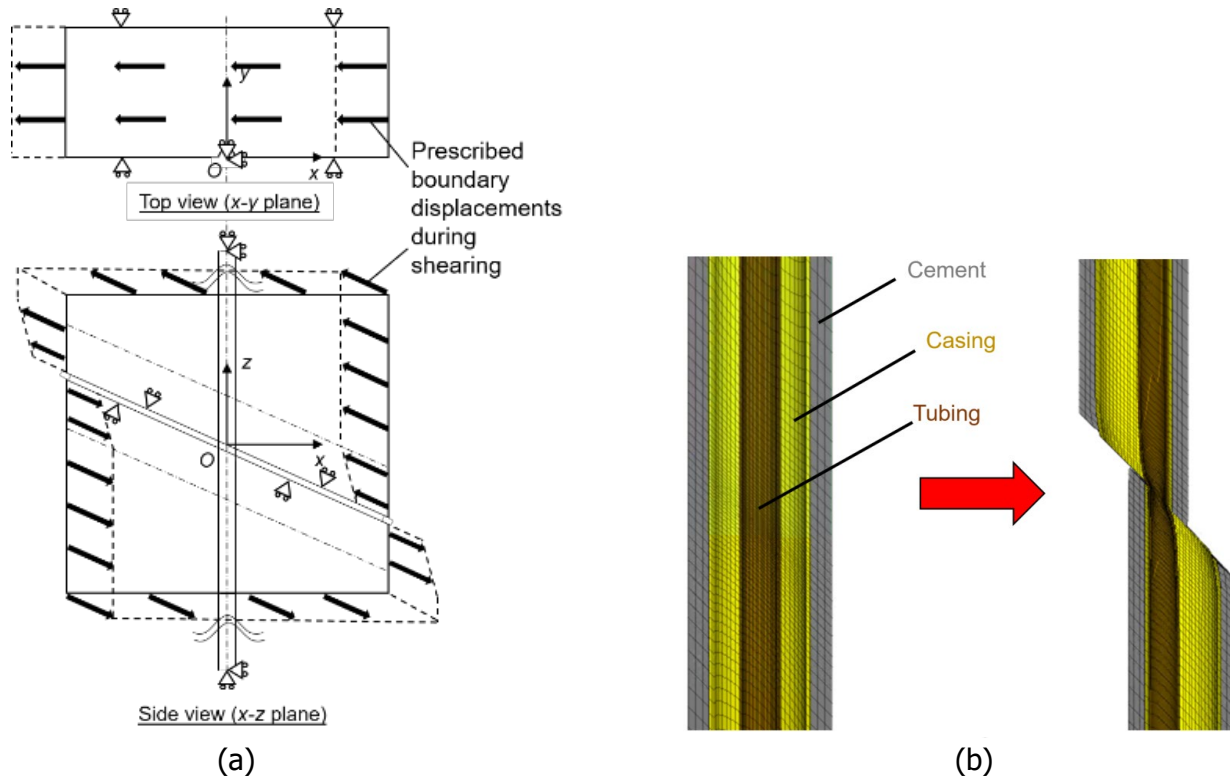
(a) Prescribed boundary displacement during shear, and (b) mesh deformation and rupture of casing and pinching of tubing during shear.

Source: Sasaki et al. (2023)

Dynamic Seismic Analysis of Well Integrity

This subtask aims to estimate the maximum bending moment a casing system can sustain when subject to earthquake-induced shaking. To do this, a site-response analysis was performed using SHAKE91 to get ground motions at 2-meter depth intervals. Then, using the open-source finite-element library OpenSeesPy v3.3 (McKenna, 2011; Zhu et al., 2018), dynamic well simulations were performed. Figure 15 shows the finite-element model used for the dynamic analysis. Within this analysis, maximum bending moment was used to describe the capacity of a casing system to withstand lateral loading. The results from the OpenSees model were used in a sensitivity study to develop damage and fragility models, outlined later in this report. The details of this model can be found in Rutqvist et al. (2022).

Figure 15: Finite-Element Conceptual Model Used in OpenSees
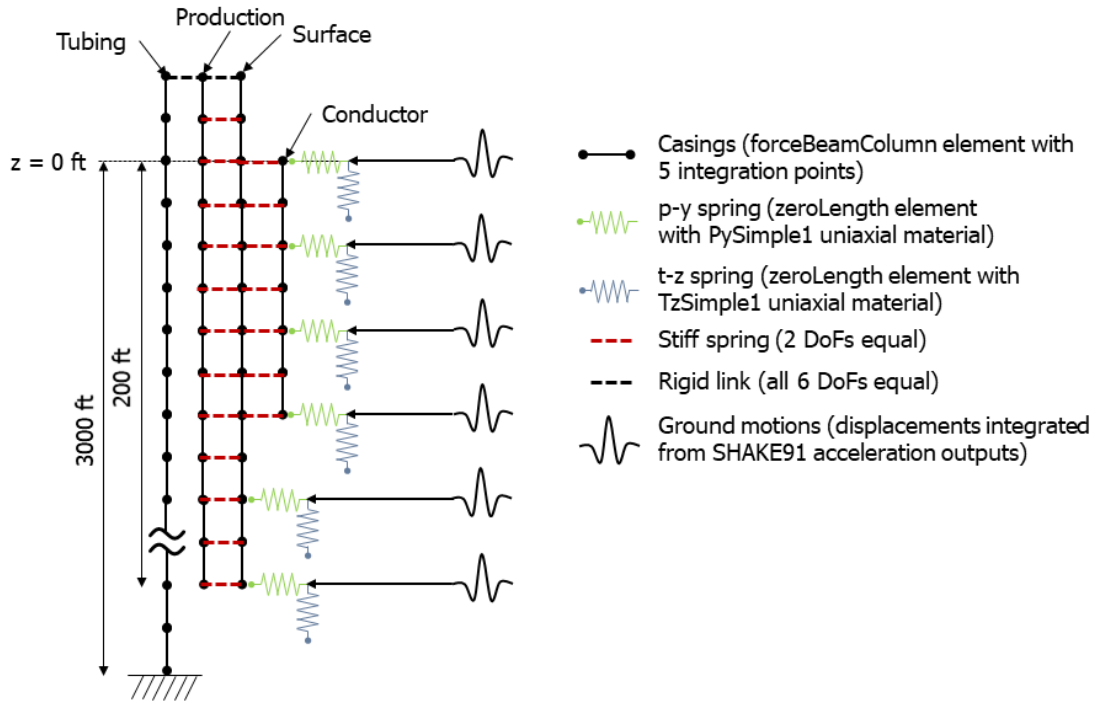
Source: Luu et al. (2023)

Caprock Integrity

In a seismic event, faults that cross a caprock could cause increased permeability if activated. This zone connects the reservoir with the formations above, creating a leakage pathway for gas to migrate upward. If the storage reservoir is also over pressured, reservoir fluid will have a driving force to migrate upwards, leading to gas loss or other environmental impacts.

This subtask first established a relationship between shear displacement and fault transmissivity; then developed a numerical model to calculate damage rates resulting from changes in fault transmissivity; assessed the depth of and pressure in a gas storage reservoir susceptible to leakage; and finally performed a suite of simulations that capture uncertainties to calculate the overall fragility of caprocks (see Rutqvist et al. [2022] for additional information regarding the literature review, statistics on caprocks, etc.).

For the numerical modelling, the TOUGH (Transport of Unsaturated Groundwater and Heat) program was used through iTOUGH2 (inverse TOUGH2). Most of the underground storage (UGS) reservoirs in California are operated far below the hydrostatic pressure (Zhang et al., 2023). Even when caprock integrity is compromised due to an earthquake, gas may not leak out due to the lack of a driving force. The Kirby Hills Domengine storage facility was found to be an exception. As such, the parameters from this storage facility were adapted in the numerical model. A schematic of the model is shown in Figure 16. The following four scenarios for this model considered in the next step to drive the fragility curve:

- The UGS reservoir and the formation above the caprock have open boundaries.

- The UGS reservoir and the formation above the caprock have closed boundaries.

- The UGS reservoir has open boundaries and the formation above the caprock has closed boundaries.

- The UGS reservoir has closed boundaries and the formation above the caprock has open boundaries.

The model output was the cumulative gas leakage over time and led to the fragility model described later in this report.

Figure 16: The Schematics of the Numerical Model for Calculating Fault Leakage
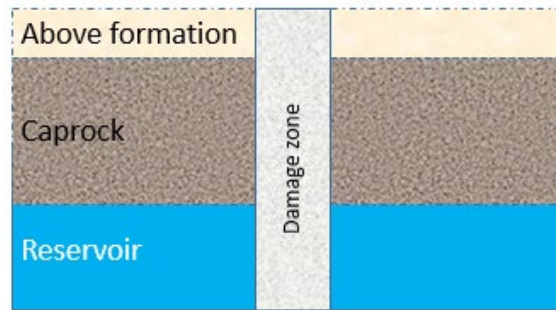
(Not to scale.)

Source: Zhang et al. (2023)

Aboveground Infrastructure

This subtask focused on developing fragility curves for different components of surficial infrastructure. The analyses in this task are split into five outcomes:

- Outcome #1: Experimental Data on Critical Components
- Outcome #2: Experimental Data Relative to Subsystems
- Outcome #3: Calibrated Nonlinear Steel Properties
- Outcome #4: Seismic Analysis of Nonlinear Subsystems
- Outcome #5: Fragility Development

Outcome #1: Experimental Data on Critical Components

Table 6 presents the test matrix for the component tests performed at the Powell Laboratories at the University of California, San Diego. Because these components behaved differently, depending on the direction of loading, select components were tested in the in-plane and out-of-plane direction.

Table 6: Test Matrix of Component Specimens

Component Type	Diameter (Schedule)	Direction of Loading	Short Name
Tee	4 in (80)	In-plane	4T-IP
	4 in (80)	Out-of-plane	4T-OP
	8 in (40)	In-plane	8T-IP
	8 in (40)	Out-of-plane	8T-OP

Component Type	Diameter (Schedule)	Direction of Loading	Short Name
90º elbow	4 in (80)	In-plane	4E-90
45º elbow	4 in (80)	In-plane	4E-45

Source: Pantoli et al. (2022)

Pre-test simulations were performed using Abaqus for each specimen, to support the development of the load protocol and instrumentation plans (Figure 17). Figure 17b shows an example of the meshed model of a specimen in Abaqus. For specifics on material type and model development, see Pantoli et al. (2022). Figure 18 through Figure 20 show the test setup for the individual components and their corresponding schematic.

Figure 17: Specimen 4T-OP

(a)

(b)
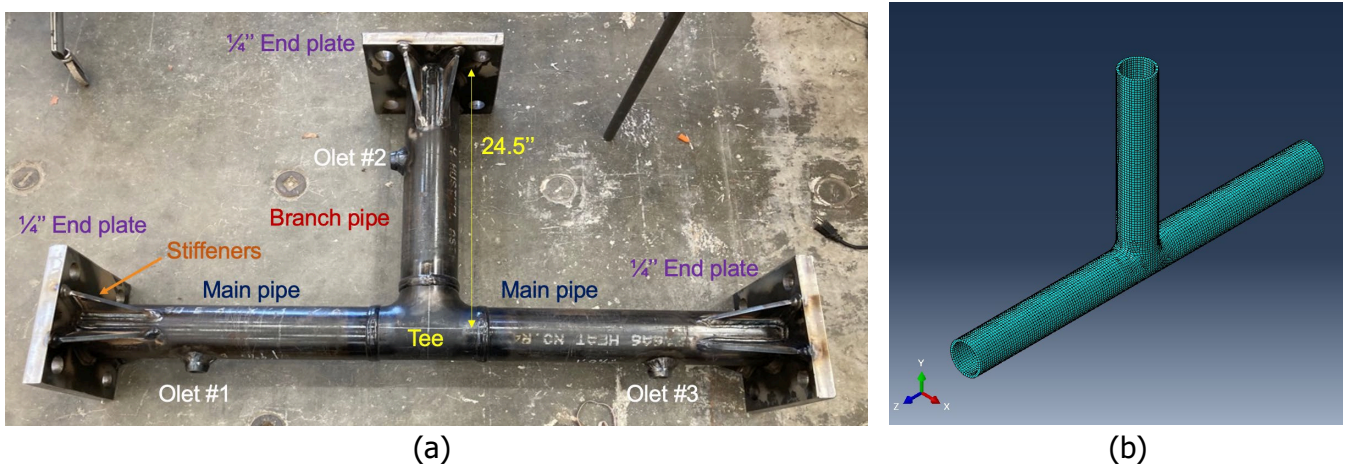
(a) Photograph, and (b) modeled and meshed in Abaqus

Source: Pantoli et al. (2022)

Figure 18: Specimen 8T-IP

(a)

(b)

26

(c)
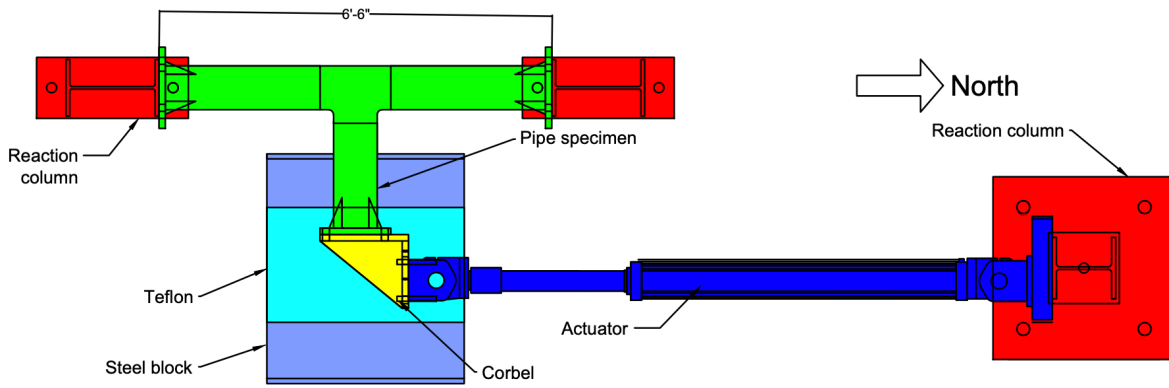
(a) and (b) Photographs, and (c) plan view

Source: Pantoli et al. (2022)

Figure 19: Specimen 4T-OP

(a)

(b)

(c)
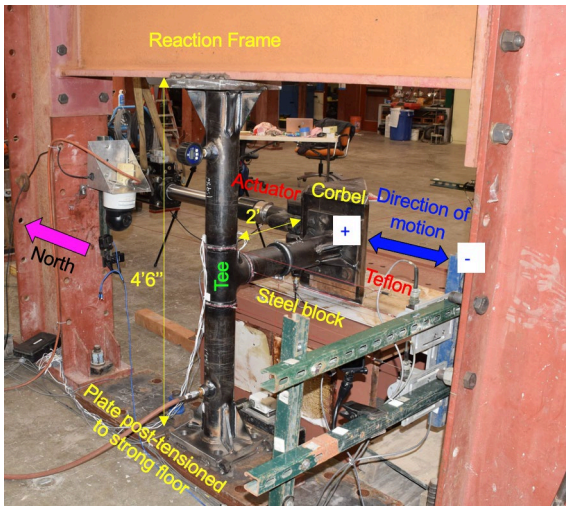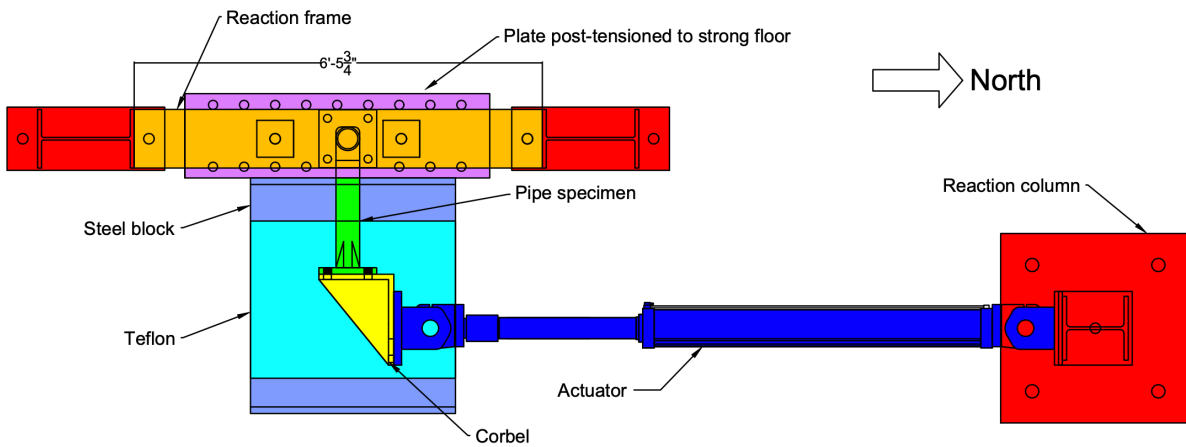
(a) and (b) Photographs, and (c) plan view

Source: Pantoli et al. (2022)

Figure 20: Specimen 4E-90

(a)

(b)

(c)
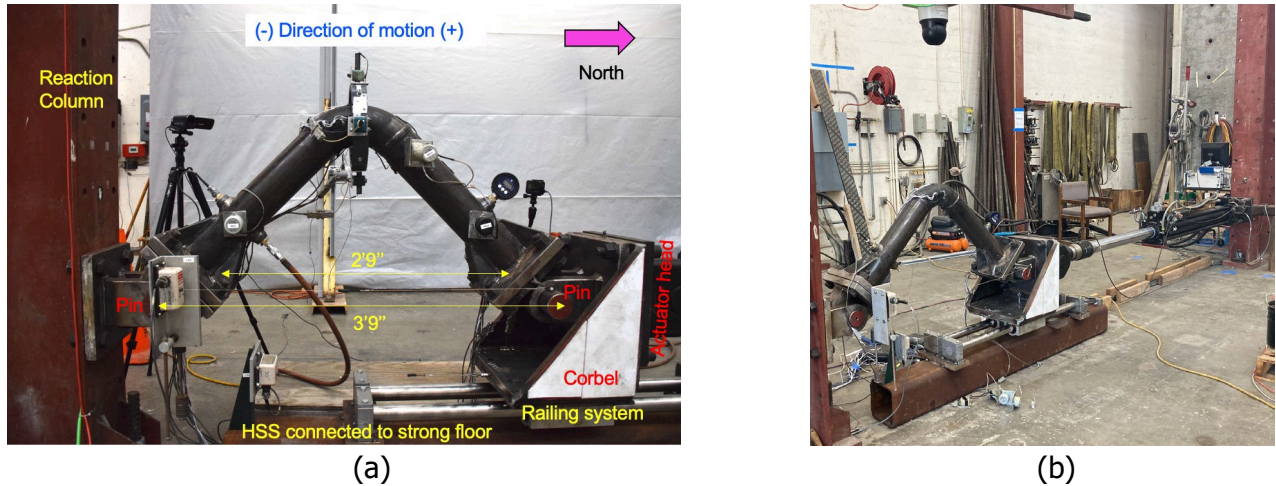
(a) and (b) Photographs, and (c) plan view

Source: Pantoli et al. (2022)

The progression of damage was the same for all the specimens except 8T-IP, and it included the following limit states:

1. First ovalization. This limit state identifies the moment when a visible deformation of the component could be observed for the first time.

2. First crack. This limit state indicates the appearance of a shallow crack at locations of high strains.

3. Through crack. A sudden loss of internal pressure happened when the continuous displacement applied to the specimen led one or more shallow cracks to become through cracks. This is considered the "failure" of the specimen.

Components failing in this way are deemed "ductile," since they show warning signs before failure happens. The only specimen that had a "brittle" failure, far from the location of high strains predicted by Abaqus, was 8T-IP.

Outcome #2: Experimental Data Relative to Subsystems

A dynamic test series was conducted on a generic (full-scale) surface infrastructure subsystem at the Earthquake Engineering Laboratory at UNR using two biaxial shake tables. Figure 21 shows a rendering of the subsystem tested at UNR, while Figure 22 shows a photograph of this subsystem and its relevant components.

Figure 21: Rendering of the Subsystem Experiment
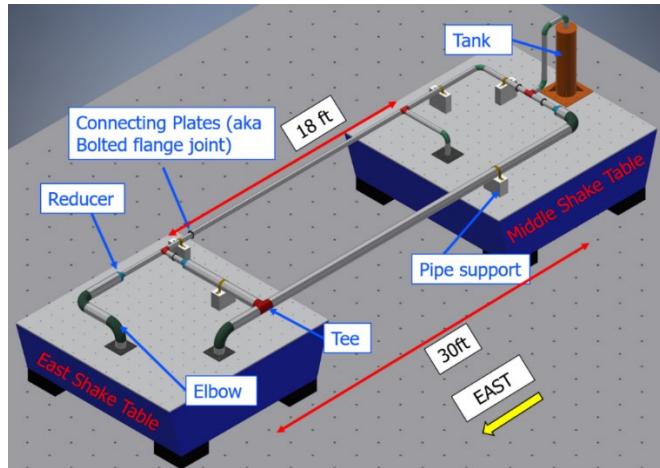
Source: Pantoli et al. (2022)

Figure 22: Photograph of the Subsystem Tested at UNR

(a)
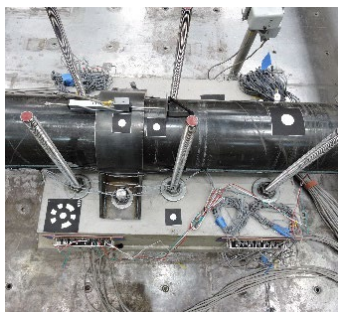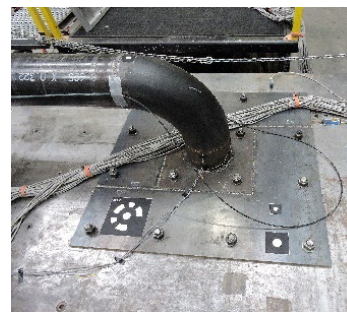
(b)(c)   (d)(e)   (d)   (e)

(a) Assembled subsystem on the UNR shake tables, (b) pipe support, (c) connecting plates, (d) elbow, and (e) vertical tank.

Source: Pantoli et al. (2022)

A nonlinear numerical model was developed before the test to gain insights on the expected behavior of the subsystem. This model was developed using OpenSees and is shown in Figure 23. Information on the validation of this model can be found in Pantoli et al. (2022). The model indicated that no damage should occur if the subsystem was subjected to uniform earthquake accelerations; however, significant deformation and yielding could occur if the subsystem was subjected to large relative displacement. Thus, the subsystem was subjected to three types of motions: broad-band white noise, synchronous motions, and asynchronous (time shifted) motions. Figure 24 shows the subsystem during testing. Figure 25 presents an example of asynchronous time motion. Information on the test setup, instrumentation, and loading protocol are provided by Elfass et al. (2023).

Figure 23: Plan View of the Pre-test Model in OpenSees

All dimensions are in inches. Red circles denote fixed supports in all degrees of freedom, green circles denote restrained supports in X and Z directions, and blue circles denote restrained supports in Y and Z directions.

Source: Pantoli et al. (2022)

Figure 24: Views From Two High-resolution Cameras

(a)

(b)

(a) Top view, and (b) side view

Source: Pantoli et al. (2022)

Figure 25: Time History of the Asynchronous Motions

(a)   (b)
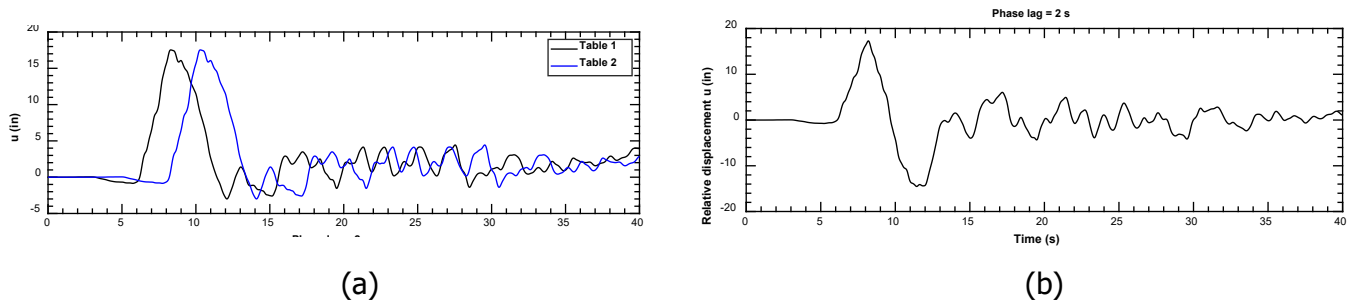
(a) Displacement time history for each shake table, and (b) time history of the resulting relative displacement between shake tables

Source: Pantoli et al. (2022)

Through these laboratory tests, it was found that only the large relative deformations caused any yielding or failure.

Figure 26 shows the progression of the behavior at relative displacements of 17 inches. The red dots denote where yielding occurred, and the number represents the ratio between the maximum strain measured at that location and the yield strain. It was also noted that the subsystem did not experience any leaks or loss of pressure. Figure 27 provides pictures of pipe deformations showing the rotation experienced by both pipelines. However, at such rotation, damage was observed to the concrete pedestal at one pipe support, as shown in Figure 28.

Figure 26: Observed Yielding at Two Cycles of Shake Table Relative Displacement
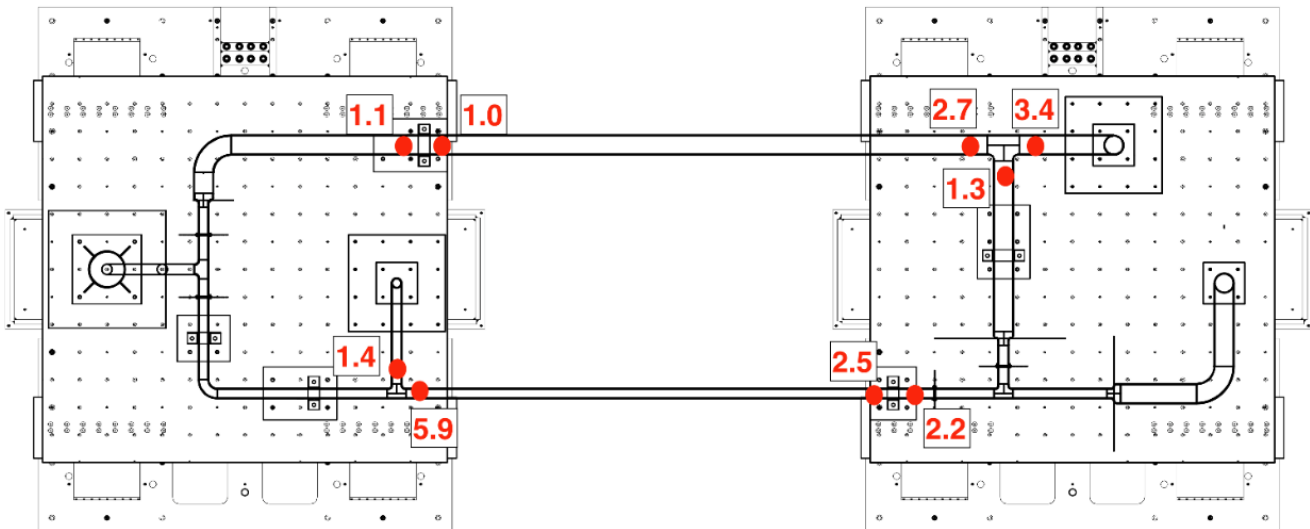
Source: Pantoli et al. (2022)

Figure 27: Piping Deformation of Relative Shake Table Displacement
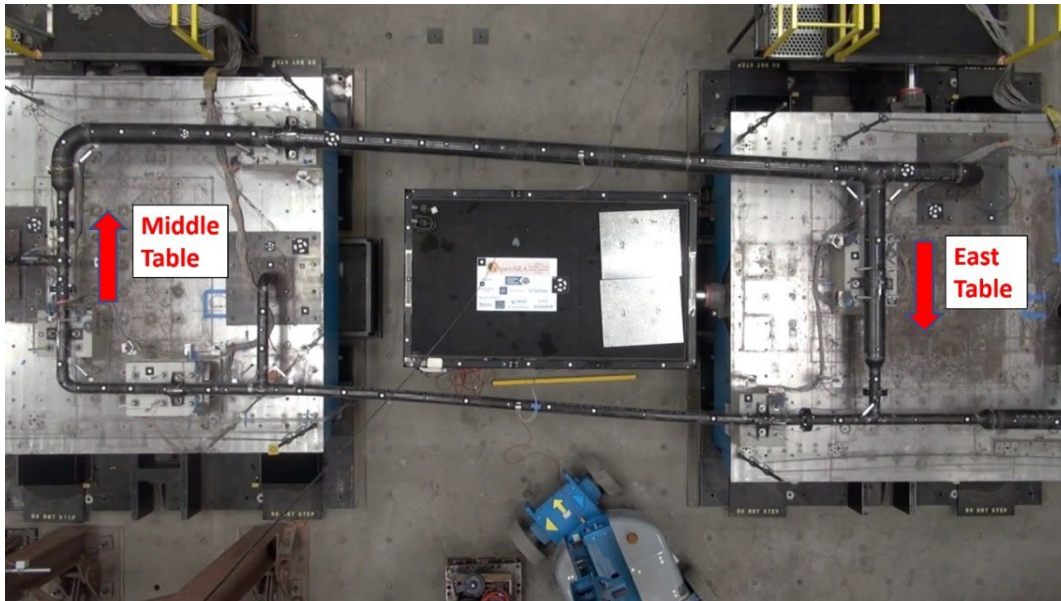
(a)
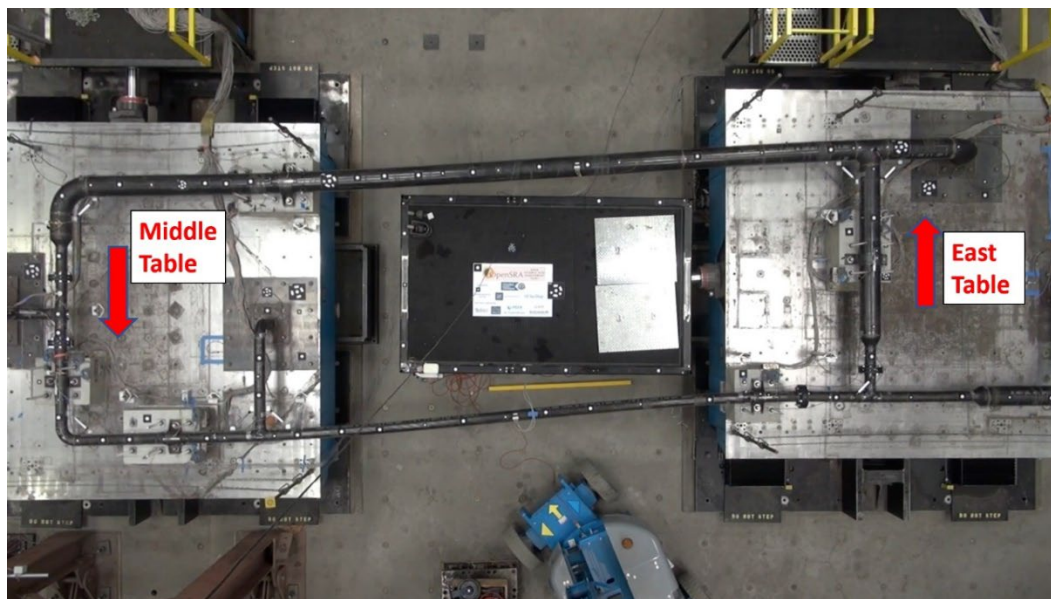
(b)

(a) Middle table moving east, and (b) middle table moving west at 17 inches.

Source: Pantoli et al. (2022)

Figure 28: Damage at a Pipe Support After the Final Motion
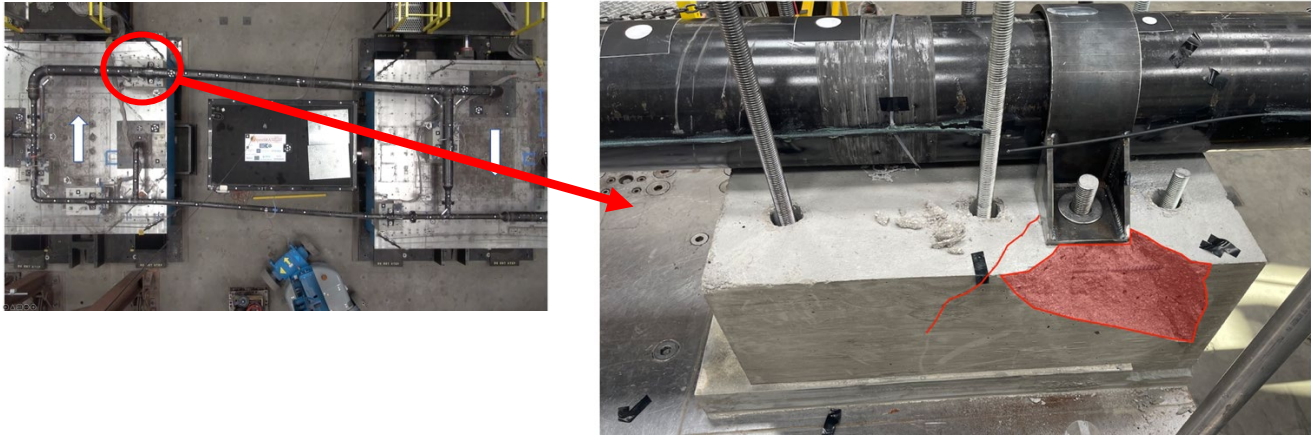
Source: Pantoli et al. (2022)

Outcome #3: Calibrated Nonlinear Steel Properties

Creating a robust and reliable nonlinear material model for steel is required for the reasonable prediction of the behavior of a steel component subjected to the large cyclic deformations that can be caused by earthquakes. To support this need, the aforementioned component experimental data were utilized in iterative form to calibrate the nonlinear material properties for the steel used for tees and elbows in the finite element models.

The optimal values of the cyclic hardening parameters were obtained by minimizing the error between the experimental results from component tests and the corresponding Abaqus numerical predictions for all specimens tested. Figure 29 and Figure 30 show example results of the calibration of these materials using a comparison of experimental and numerical results. Further information about the validation process can be found in Pantoli et al. (2022).

Figure 29: Comparison of Numerical and Experimental Moment-rotation Curves

(a)   (b)
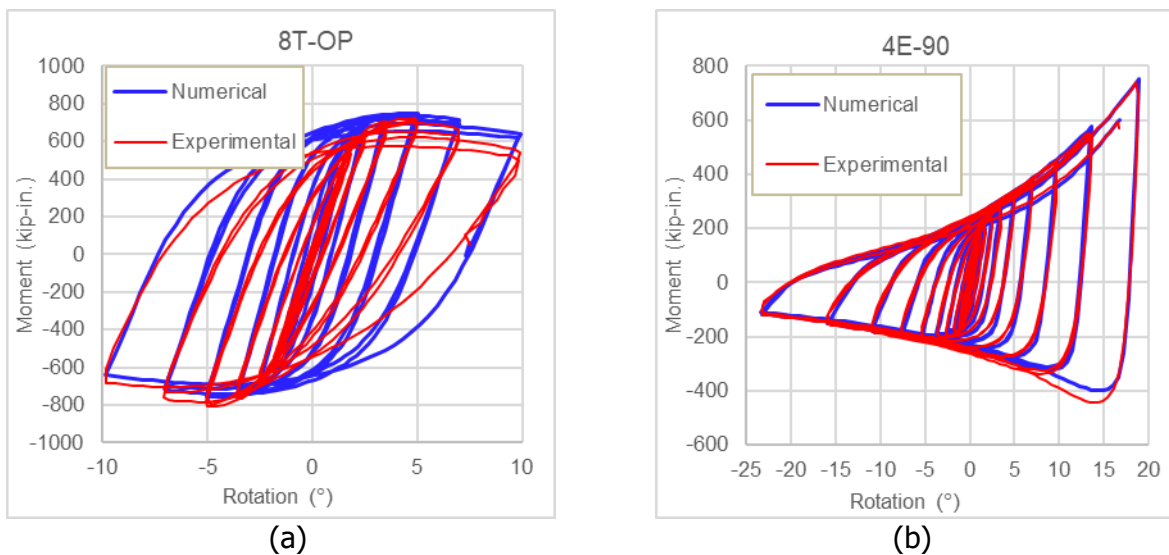
(a) Specimen 8T-IP, and (b) specimen 4E-90

Source: Pantoli et al. (2022)

Figure 30: Comparison of Numerical and Experimental Time History of Moment

(a)

(b)
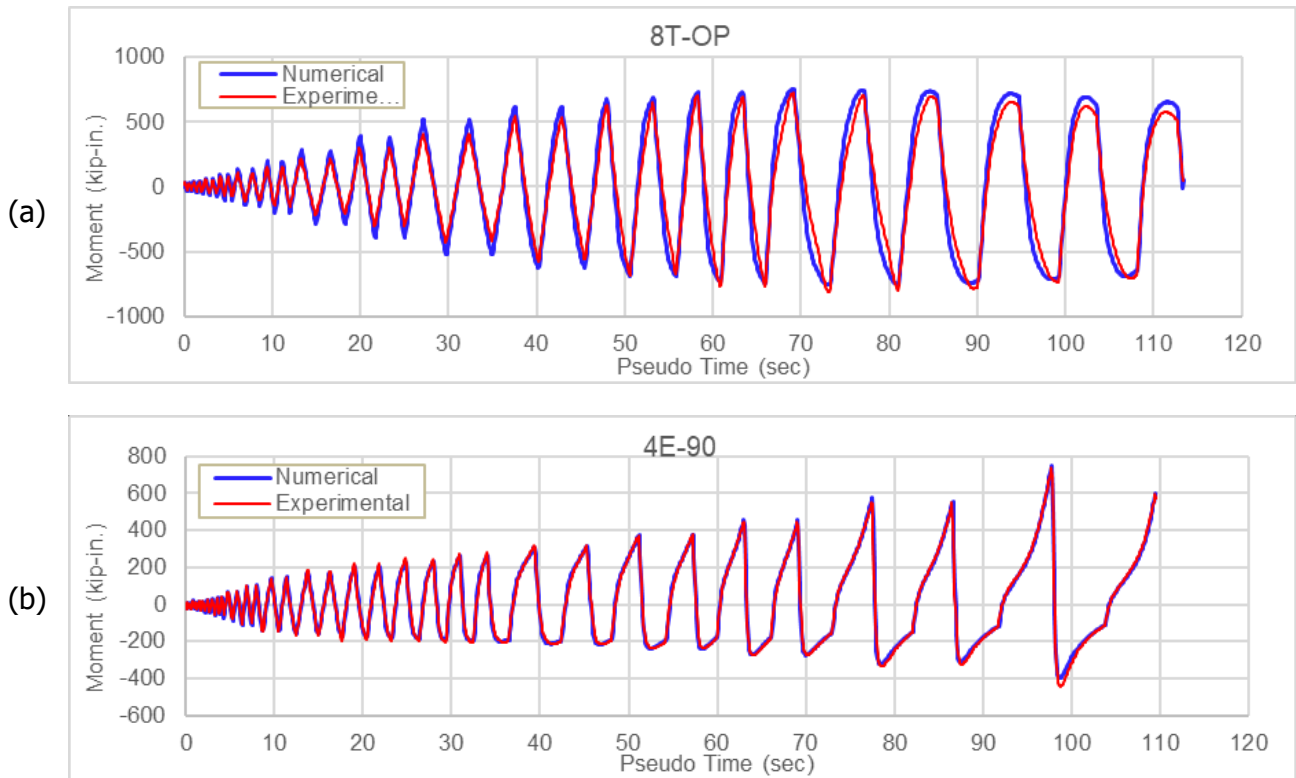
(a) Specimen 8T-IP, and (b) specimen 4E-90

Source: Pantoli et al. (2022)

Outcome #4: Seismic Analysis of Nonlinear Subsystems

Task Group D developed a procedure for the seismic analysis of nonlinear gas subsystems using OpenSees that can be used to generate fragility curves for *OpenSRA*. In this procedure, the nonlinearities and failure points of the subsystem are concentrated at the location of critical components, while the remainder of the model subsystem remains linear. The subsystems explored are the wellhead tree-pipeline (WTP) subsystem, where buried pipelines come to the surface and end in a wellhead that then distributes the gas aboveground, and vertical pressure vessels (VPV). The geometry of these subsystems is based on photographic evidence found on public resources, design calculations, manufacturer catalogues of valves and other components, site visits to a gas storage facility, and personal communication with experts at utility companies.

WTP Subsystem

A typical wellhead tree is depicted in Figure 31(a) and the corresponding OpenSees model used for fragility development is shown in Figure 31(b). Further information regarding wellhead trees and their geometry in California and validation of the OpenSees model can be found in Pantoli et al. (2022).

Figure 31: Wellhead Tree

(a)   (b)
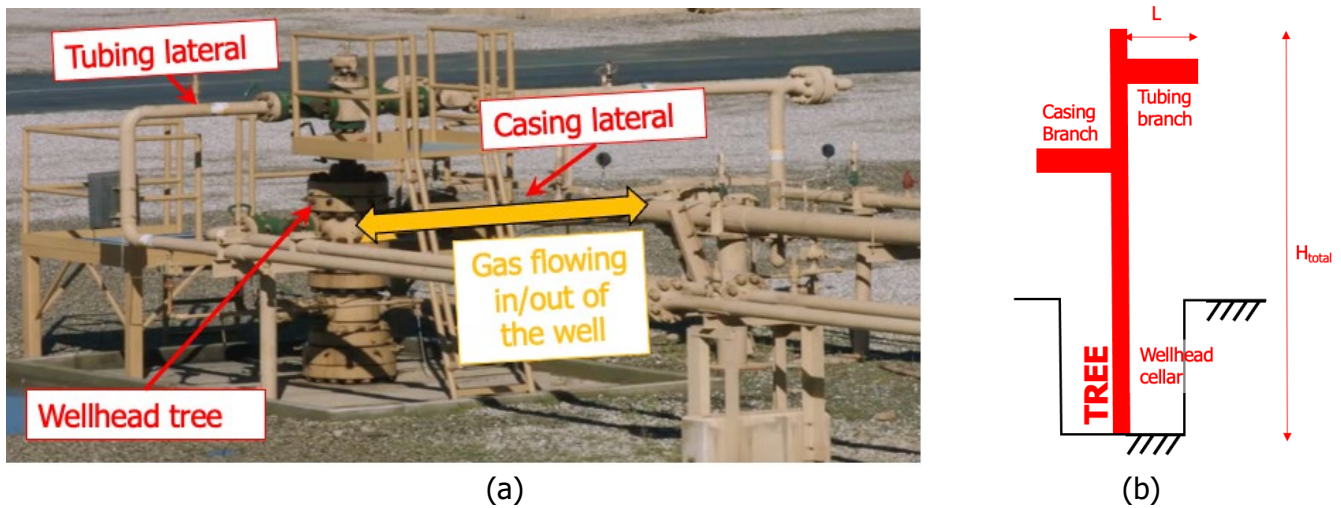
(a) Photograph of a wellhead tree and connected piping, and (b) schematic of a wellhead tree showing relevant nomenclature

Source: Edited from SoCalGas (2016)

The procedure used to calibrate the parameters of this model in OpenSees involved the following elements:

- A numerical model of the critical components and sections of straight pipes was created in Abaqus. This model used the calibrated material properties obtained in Outcome #3 and the field boundary conditions. The Abaqus model of the tee rotating in-plane is shown in Figure 32(a).

- An OpenSees model of the same geometry and boundary conditions was created, as shown in Figure 32(b).

- The two models were subjected to the same displacement-controlled cyclic analysis with a load protocol.

- The forces necessary to obtain this displacement in the Abaqus and OpenSees were compared.

This same procedure can be used to extend the results to a wider range of component types/details and loading conditions. As an additional step in validation, impact tests were performed at a gas storage field in California; additional information on these tests can be found in Pantoli et al. (2022).

Figure 32: Component Models for the Tee Rotating In-plane

(a)   (b)
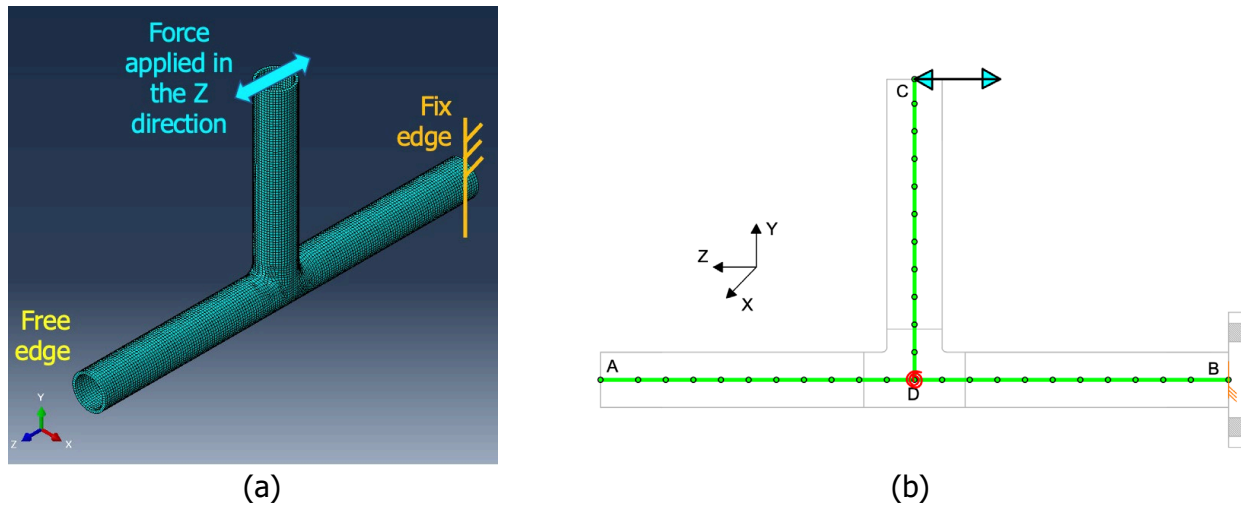
(a) Abaqus model, and (b) OpenSees model

Source: Pantoli et al. (2022)

VPV Subsystem

The vertical pressure vessels observed at gas storage facilities comprise a tall cylindrical vessel with hemispherical or elliptical heads supported by a skirt, as shown in Figure 33(a). The optimal EDP for these analyses is the ratio between the moment demand at the base imposed by an earthquake and the moment capacity at which a limit state is achieved.

Validation of the VPV Subsystem

For the validation of this subsystem, a sample VPV geometry was selected based on representative information of a pressure vessel provided by a gas company in California. This sample VPV was modeled using Abaqus and a complimentary but simplified linear version utilizing 1D finite elements within OpenSees. These results showed that:

- The movement of the pressure vessel itself was not affected by the movement of the pipes.

- The inlet pipe connected to the bottom of the pressure vessels had minimal movement in these lower frequency modes.

- The simplified OpenSees model could capture the behavior of this subsystem predicted by the more refined Abaqus model.

Figure 33: Vertical Pressure Vessels
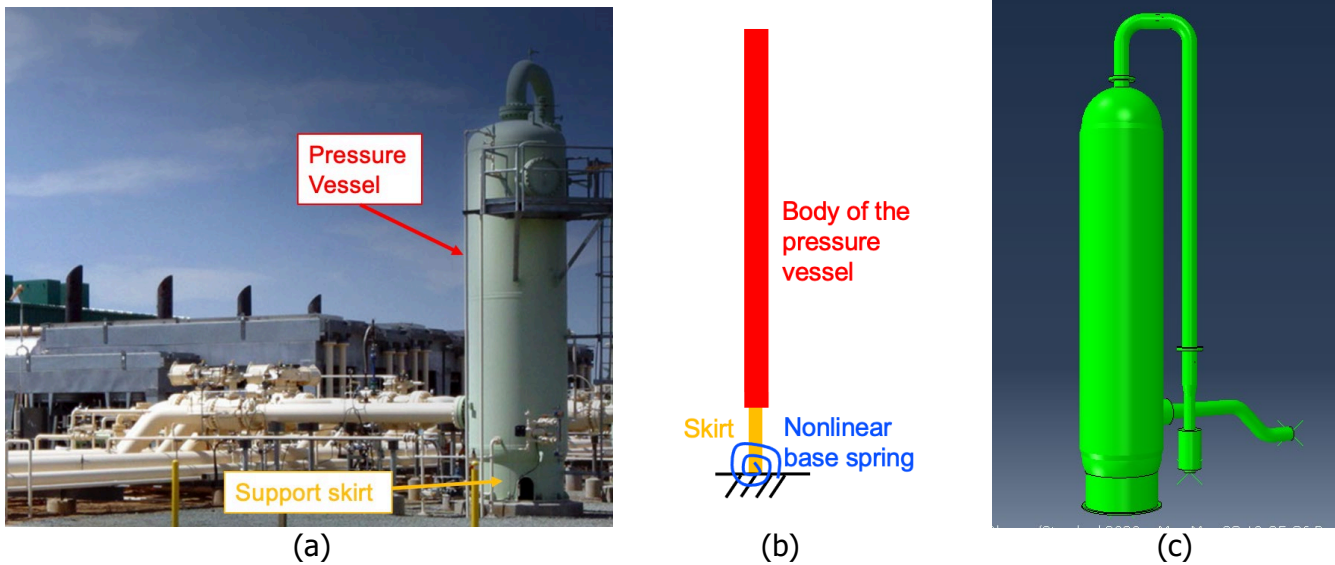
(a) Photograph of RockPoint Gas Storage, 2021, (b) schematic of the OpenSees Model, and (c) Abaqus model

Source: Pantoli et al. (2022)

Outcome #5: Fragility Development

The final fragility functions developed for Outcome #5 are fully presented in Watson-Lamprey et al. (2022). The following includes a sample of the damage model curves developed for 4T-IP at no pressure and high pressure; these are presented in blue and orange in Figure 34. The polynomial curves were obtained by interpolating the relevant points.

Figure 34: DM(EDP) Curves for 4T-IP
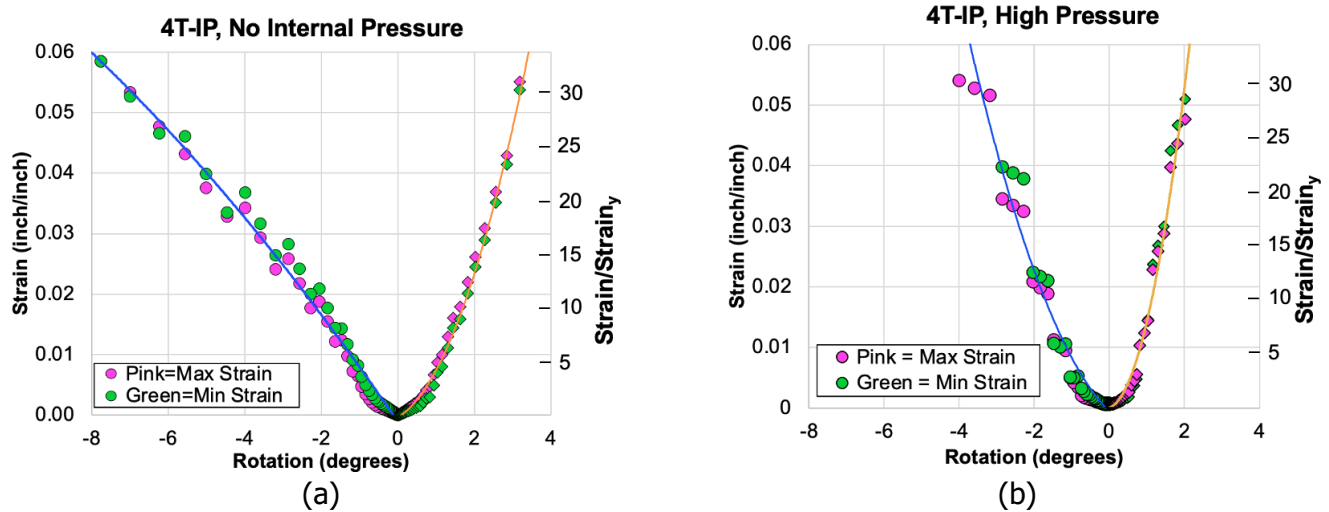
(a) No internal pressure, and (b) high internal pressure

Source: Pantoli et al. (2022)

Sensing Technologies

This task identified the technologies that can inform the risk models at the input, intermediate, and final output stages.

The sensing technologies introduced in Wang et al. (2021) were selected depending on *OpenSRA* parameters, which include geologic information and characteristics of the gas infrastructure. The selected sensing technologies can be categorized into four main categories:

1. Remote sensing technologies
2. Continuous monitoring technologies
3. Inspection technologies
4. Leakage detection technologies

Remote Sensing Technologies

Ground deformation is an important input in *OpenSRA*, regardless of the level of analysis. Remote sensing technologies have been used widely to detect and monitor objects (including ground deformation). Table 7 presents a comparison of these technologies and their uses.

Table 7: Comparisons of Remote Sensing Technologies

Technology	Advantages	Disadvantages	Occasions
LiDAR	Highest accuracy; able to penetrate vegetation	Cannot penetrate fog and rain; high cost	Most cases, except during fog or rain
InSAR	Accurate; available for most cases	High cost	Most cases
Aerial and satellite photography	Relatively low cost	Need line of sight	Low-vegetation area or vegetation height is considered, and without fog and rain

Source: Wang et al. (2021).

Continuous Monitoring Technologies

Continuous monitoring technologies are deployed on site and operate on stand-alone power and cellular communication. The selected continuous monitoring technologies include distributed fiber optic sensors (DFOS) and wireless sensor network (WSN). Table 8 and Figure 35 specifically outline uses of WSN; and more information regarding DFOS and the tests done within this project can be found in Wang et al. (2021).

Table 8: Wireless Sensor Network Based Sensing Technologies and the Corresponding Events and Occasions

Technologies	Events	Occasions
Soil moisture sensor	Leakage	Underground pipeline
Accelerometer	Leakage	All
Strain gauge	Deformation	All

Technologies	Events	Occasions
Position sensor	Relative displacement	Aboveground pipeline
Flow sensor	Leakage	All
Gas sensor	Leakage	Mostly aboveground

Source: Wang et al. (2021).

Figure 35: WSN Instrumentations

(a)

(b)
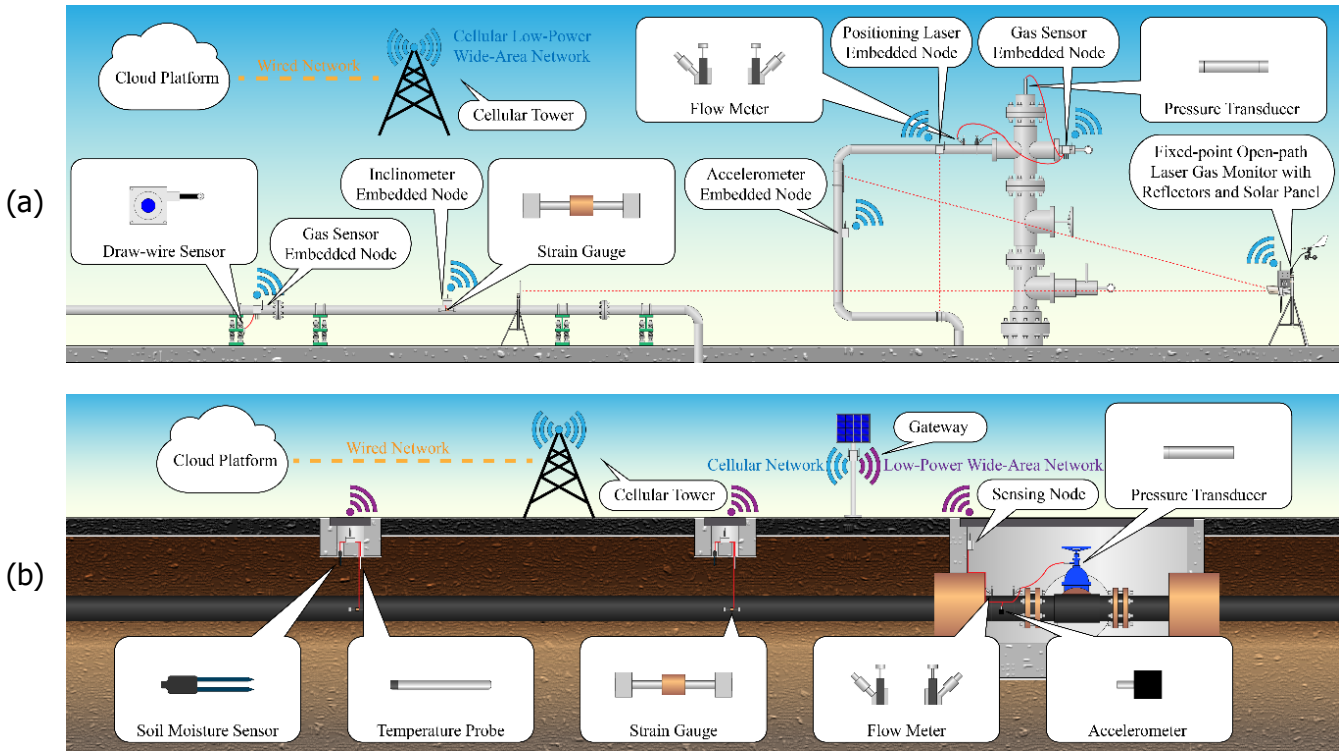
(a) Aboveground and (b) underground gas pipeline monitoring

Source: Wang et al. (2021).

In-line Inspection Technologies

Inspection technologies specifically help identify pipeline characteristics from inside the pipe. These characteristics can be used as a reference for inputs and to verify the intermediate and final outputs of *OpenSRA*. This project focused on the in-line inspection techniques that can be done at the same time as the periodical pigging progress. Table 9 compares different in-line inspection technologies and their applications.

Table 9: Associable Sensing Technologies for Smart Pig

Technology	Application
Magnetic Flux Leakage	Surface pitting, corrosion, cracks, and weld defects detection (for steel/ferrous pipelines only)
Ultrasonic	Cracks, coating, and lamination defects detection
Caliper	Bending and other deformations

39

Technology	Application
Temperature Sensor	Providing the indication of the likely type of debris present
Odometer	Providing the travel distance of the pig
Orientation Sensor	Providing the travel direction of the pig
Vibration Sensor	Providing position fixing at each joint

Source: Wang et al. 2021.

Leakage Detection Technologies

Gas and flow sensing technologies help characterize leakage events and provide information on the amount of the leakage. This helps utility owners focus mitigation efforts after a seismic event occurs. This project introduced different types of gas and flow sensors, including their mechanisms, abilities, limitations, and comparisons, as a reference for helping users select the sensors that best suited their applications (Table 10).

Table 10: Comparison of Gas Flow Monitoring Technologies

Technology	Advantages	Disadvantages	Occasions
Coriolis	High accuracy and turn-down ratio, independent of fluid properties and entrained gases	Expensive to purchase and install, pressure drop, not suitable for large pipe size	Small pipe sizes, changing conditions
Thermal mass	High accuracy and repeatability, easy to install	Very low response time, dry and clean fluids	Dry and clean fluids
Turbine	Very high versatility and accuracy, fast response time, high pressure and temperature capabilities	Moving parts can wear or clog, not suitable for low flow rate	Not for low flow, viscous, dirty, and corrosive fluids
Ultrasonic	Very high versatility and accuracy, no pressure drop, low maintenance, non-invasive	Expensive, not suitable for low flow rate	Not for low flow
Vortex	Low pressure drop, high versatility and pressure capability	Limited by viscosity and minimum flow rate, needs temperature and pressure compensation, no entrained solid and gas	Clean gas, high pressure, low viscous fluids
Differential pressure	Flexible specification, experienced and reliable, generally low cost	Limited range ability, complex installation	Most occasions

Technology	Advantages	Disadvantages	Occasions
Positive displacement	Very high versatility, accuracy, and turndown ratio; reliable	Moving parts can wear or clog, needs temperature and pressure compensation, pressure drop	Most occasions (includes viscous, dirty, and corrosive fluids)

Source: Wang et al. (2021).

OpenSRA Informing Technologies Guidance

Measured data (as seen in the laboratory testing in previous sections) aid in the industry's understanding of how a system reacts, specifically in a seismic event. Leveraging this measured data will continue the progress made in this project to update current risk models. Implementing sensing technologies now will aid the industry in decision making and risk mitigation in the future. The following tables outline how different sensing technologies can improve the analyses on specific gas infrastructure.

Gas Pipelines

The pipeline response estimate requires both infrastructure and geotechnical characteristics. Table 11 shows examples of the required input as well as the intermediate and final output parameters used with this tool.

Table 11: Gas Pipeline Simulation Tool Parameters

Variables		Description	Unit	Available Tech
INPUT	Structural	Pipe outside diameter	mm	Ultrasonic, Magnetic Flux Leakage with caliper
		Pipe wall thickness	mm	Ultrasonic, Magnetic Flux Leakage
		Pipe yield stress	kPa	-
		Ramberg-Osgood parameter	UNIT-LESS	-
		Ramberg-Osgood parameter	UNIT-LESS	-
	Geotechnical	Total unit weight of backfill soil	kN/m3	-
		Soil cover to centerline of pipeline	m	-
		Length of ground deformation zone	m	LIDAR
		Backfill friction angle	Degree °	-
		Sand/pipe interface friction angle ratio	UNIT-LESS	-
		Permanent ground deformation	m	LIDAR, InSAR, Structure from Motion

	Variables	Description	Unit	Available Tech
INTERMEDIATE		Force per unit length of pipeline	kN	DSS, WSN (Strain gauge)
		Pipe burial parameter	kPa	-
		Embedment length	m	-
		Standard deviation of Le estimate (ln units)	-	-
		Value of L to use in pipe strain equation	-	-
OUTPUT		Pipe strain	%	DSS, WSN (Strain gauge)
		Standard deviation of pipe strain estimate (ln units)	-	-
		Epistemic uncertainty	-	-

All variables and references used for descriptions in this table correspond to the Task B report.

Source: Wang et al. (2021).

Gas Storage Wells

The well characteristics and ground conditions are required by the gas storage wells response estimate. Table 12 shows examples of the required input and the generated intermediate and final output parameters used in this tool.

Table 12: Gas Storage Wells Simulation Tool Parameters

	Variables	Description	Unit	Available Tech
INPUT	Casing and Tubing	Casing-tubing interface friction coefficient	-	-
		Casing pressure	MPa	WSN (pressure sensor)
		Young's modulus of casing/ tubing	GPa	-
		Density of casing/tubing	kg/m3	-
		Poisson's ratio of casing/tubing	-	
		Internal friction angle of cement	Degree °	-
		Uniaxial compressive strength of cement	MPa	-
		Tensile strength of cement	MPa	-
		Yield strength of casing/tubing	Ksi	-
		Yield/Tensile strength ratio of casing/tubing	-	-

	Variables	Description	Unit	Available Tech
	Wellhead	Wellhead mass per length	kg/m [lb/in]	-
		Wellhead height	m [ft]	LIDAR, Structure from Motion, WSN (displacement)
	Geotechnical	Fault angle	Degree °	-
		Fault core width	m	-
		Damage zone width	m	-
		Depth of fault-well intersection	m	-
		Maximum horizontal-to-vertical effective stress ratio	-	-
		Young's modulus of rock	GPa	-
		Density of rock	kN/m3	-
		Permanent ground deformation	m	LIDAR, InSAR, Structure from Motion
INTER-MEDIATE		Fault displacement	m	LIDAR, InSAR, Structure from Motion
OUTPUT		Pipe strain	%	DSS, WSN (Strain gauge)
		Pipe bending moment	kN-m [lbs-ft]	DSS, DAS
		Standard deviation of pipe strain estimate (ln units)	-	-
		Epistemic uncertainty	-	-

All variables and references used for descriptions in this table correspond to the Task C report.

Source: Wang et al. (2021).

Aboveground Gas Infrastructure

The infrastructure response estimate requires the characteristics of the target infrastructural components, which include pipes, elbows, tee joints, vessels, outlet, and inlet pipes. Table 13 shows examples of the required input and generated final output parameters used in this tool.

Table 13: Aboveground Gas Infrastructure Simulation Tool Parameters

	Variables	Description	Unit	Available Tech
INPUT	-	Pipe yield stress	MPa [psi]	-
	Pipes	Outside diameter of the pipeline	mm [inch]	LIDAR, Ultrasonic, Magnetic Flux Leakage with caliper

Variables		Description	Unit	Available Tech
		Wall thickness of the pipeline	mm [inch]	Ultrasonic, Magnetic Flux Leakage
	Elbows	Outside diameter of the pipeline	mm [inch]	LIDAR, Ultrasonic, Magnetic Flux Leakage with caliper
		Wall thickness of the elbows	mm [inch]	Ultrasonic, Magnetic Flux Leakage
	Tees	Outside diameter of the tees	mm [inch]	LIDAR, Ultrasonic, Magnetic Flux Leakage with caliper
		Wall thickness of the tees	mm [inch]	Ultrasonic, Magnetic Flux Leakage
	Vessel	Total height of the pressure vessel	m [ft]	LIDAR, Structure from Motion, WSN (displacement)
		Diameter of the pressure vessel	-	LIDAR, Structure from Motion
		Design pressure for the vessel (used to calculate thickness)	-	-
		Vessel thickness	mm [inch]	Ultrasonic, Magnetic Flux Leakage
	Outlet Pipe	Height of joint 1 of outlet pipe	%	LIDAR, Structure from Motion, WSN (displacement)
		Length of segment LO12	%	LIDAR, Structure from Motion, WSN (displacement), DSS
		Length of segment LO23	%	LIDAR, Structure from Motion, WSN (displacement), DSS
		Height of joint 4 of outlet pipe	m [ft]	LIDAR, Structure from Motion, WSN (displacement)
		Length of segment LO45	m [ft]	LIDAR, Structure from Motion, WSN (displacement), DSS
		Type of joint at node 4 for outlet pipe	-	-
		Type of joint at node 5 for outlet pipe	-	-
	Inlet Pipe	Height of joint 1 of inlet pipe (% of Hpv [0-1])	%	LIDAR, Structure from Motion, WSN (displacement)
		Length of segment LO12 (% of Dpv)	%	LIDAR, Structure from Motion, WSN (displacement), DSS
		Type of joint at node 5 for inlet pipe	-	-

Variables		Description	Unit	Available Tech
	Wellhead Tree	Total height of the wellhead aboveground	m [ft]	LIDAR, Structure from Motion, WSN (displacement)
		Height of the horizontal section	m [ft]	LIDAR, Structure from Motion, WSN (displacement)
		Average stiffness of the wellhead	kN/m [kip/inch]	-
		Linear mass of the wellhead tree	kg/m [kip/inch]	-
		Length of segment LP_0-1	m [ft]	LIDAR, Structure from Motion, WSN (displacement), DSS
		Length of segment LP_1-2	m [ft]	LIDAR, Structure from Motion, WSN (displacement), DSS
		Length of segment LP_2-3	m [ft]	LIDAR, Structure from Motion, WSN (displacement), DSS
		Length of segment LP_3-4	m [ft]	LIDAR, Structure from Motion, WSN (displacement), DSS
		Type of joint at node 1	-	-
		Type of joint at node 2	-	-
		Type of joint at node 3	-	-
		Type of joint at node 4	-	-
OUTPUT		Strains	%	DSS, WSN (Strain gauge)
		Epistemic uncertainty	-	-

All variables and references used for descriptions in this table correspond to the Task D report.

Source: Wang et al. (2021).

Synthesis of Component Fragilities Into a System Performance Model

Buried Pipelines

Figure 36 presents the suggested lognormal cumulative distribution functions for the tensile strain damage state fragility functions, assuming a constant aleatory variability, $\sigma = 0.30$, for both leakage and rupture, which was estimated using expert opinion (Abrahamson, 2022). The 10th and 90th percentiles are presented for the fragility functions, assuming constant epistemic uncertainty, $\sigma_{epi}=0.20$, a common assumption for structural systems. Here, σ represents the aleatory variability in the fragility models due to inherent randomness in the loading conditions (e.g., eccentricities in the pipe alignment, nonuniform backfill soil conditions) and pipe properties (e.g., post-yield stress-strain behavior, weld quality, corrosion). To account for the greater uncertainty associated with field conditions, the aleatory variability, σ, was increased from 0.407 to 0.50.

Figure 36: Tensile Damage State Fragility Model
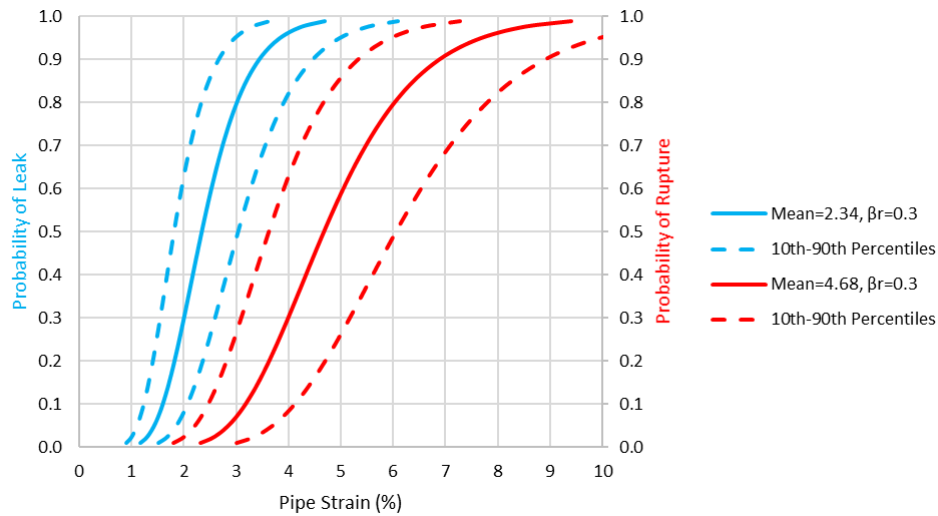
Source: Watson-Lamprey et al. (2022).

Pipelines can often sustain more axial strain after the initiation of buckling or pipe wall wrinkling before pipe wall tearing or rupturing occurs. The probability of compressive rupture (due to buckling or pipe wall wrinkling) fragility function accounts for this additional capacity by shifting the 50% probability of exceedance values in the original fragility function up to the 20% probability of exceedance level in the final function. Additional details of the pipeline fragility models are provided in Appendix D in Bain et al. (2022). Figure 37 depicts the fragility model for compressive ruptures.

Figure 37: Probability of Compressive Rupture for Select D/t Ratios
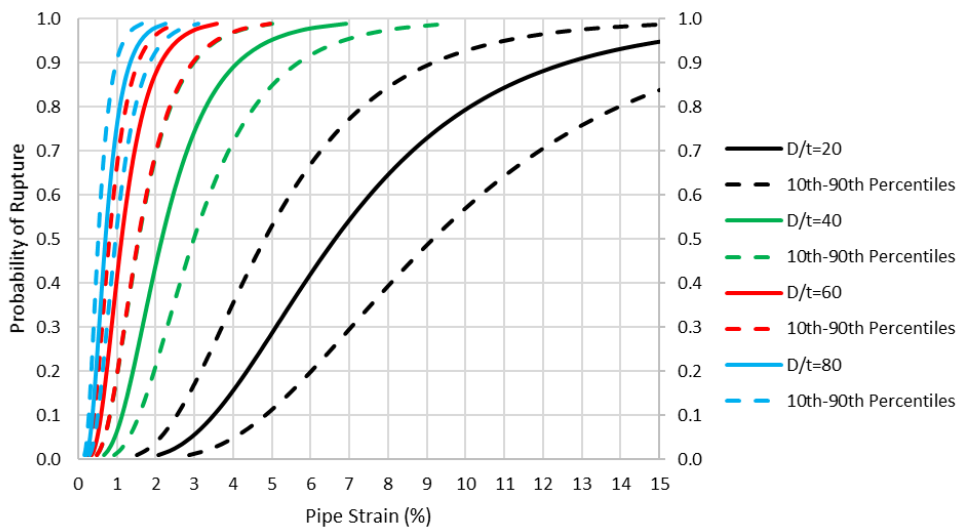
Source: Watson-Lamprey et al. (2022).

Fault Shear-Induced Failure on Wells

The probability of failure given fault-displacement-induced shear strain is presented in Figure 38.

Figure 38: Probability of Failure for Well Casing and Tubing Due to Fault Offset
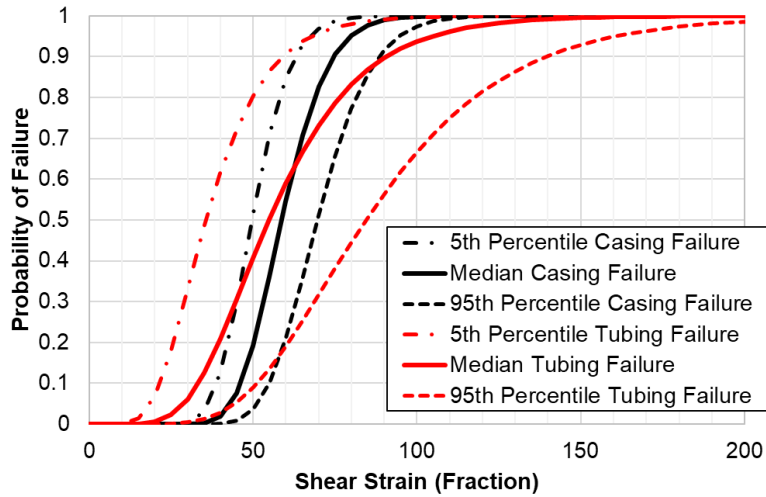
Source: Watson-Lamprey et al. (2022).

Shaking-Induced Failure on Wells

The probability of ground shaking-induced failure is plotted in Figure 39 through Figure 42 for the conductor casing, production casing, surface casing, and well tubings. The median plastic moment at which 50 percent probability of failure occurs was compiled and estimated by the Task C researchers.

Figure 39: Probability of Failure for Conductor Casing Due to Ground Shaking
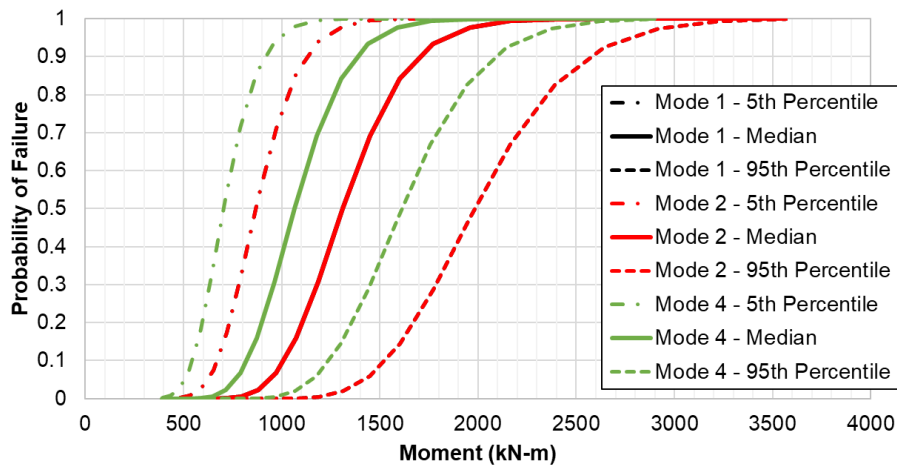
Source: Watson-Lamprey et al. (2022).

Figure 40: Probability of Failure for Surface Casing Due to Ground Shaking
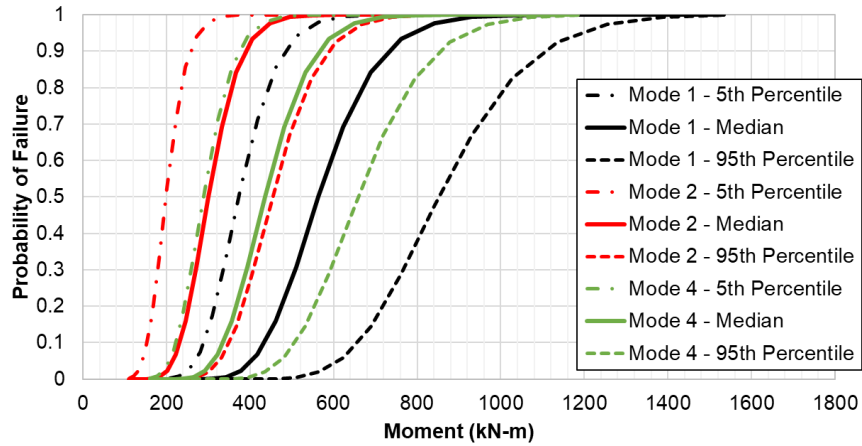
Source: Watson-Lamprey et al. (2022).

Figure 41: Probability of Failure for Production Casing Due to Ground Shaking
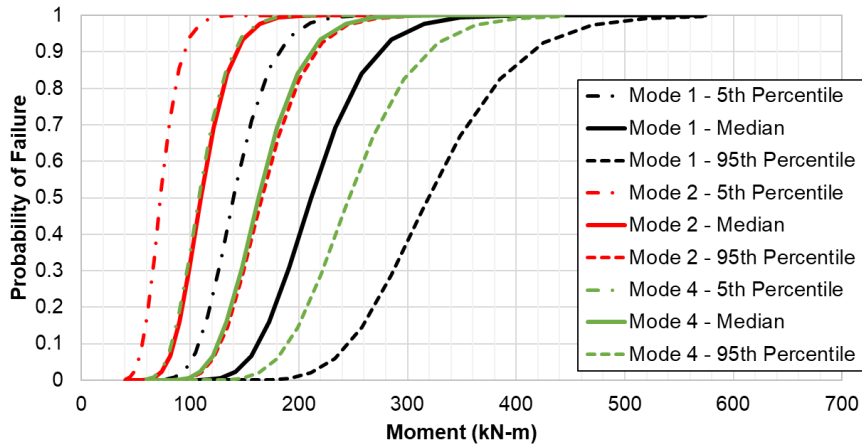
Source: Watson-Lamprey et al. (2022).

Figure 42: Probability of Failure for Tubing Due to Ground Shaking
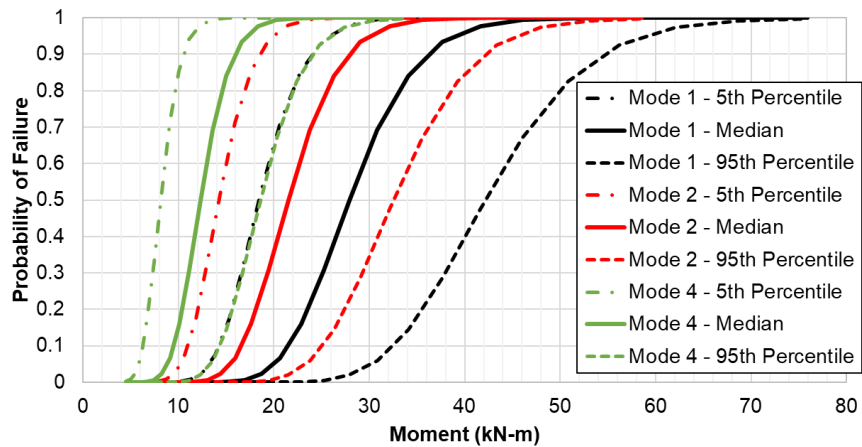
Source: Watson-Lamprey et al. (2022).

Fault Shear-Induced Failure on Caprocks

Based on the finite element modeling performed under Task C, caprocks proved to be insensitive to most of the input parameters. As such, the only parameter taken into account is if a fault crosses the caprock. If caprock-fault crossing exists, then the average probability of leakage for caprocks is 8.9%, with σ_{epi} of 0.86 percent.

Aboveground Systems

The models for failure of aboveground components are dependent on ground shaking. As seismic hazards are distributed over an area, all aboveground components that were within 200 kilometers of each fault trace would be evaluated for ground shaking-induced failure.

Well Tree

As described previously and in Watson-Lamprey et al. (2022), methodologies for probability of failure provided for well trees fall into six cases; these cases are further split based on direction of ground motion. In total, there were 22 unique models that may have needed to be computed to the distribution of joint rotation over the six subsystem-component combinations. Each of the rotation models was then propagated into models for longitudinal strain and, subsequently, the probability of failure given longitudinal strain. Once the probability of failure for a specific subsystem-component combination, direction of shaking, joint location, and orientation was determined, then the distributions of probability of failure for all variations within each subsystem-component combination were averaged to obtain the overall average distribution for probability of failure. Figure 43 shows the probability of failure for wellheads due to ground shaking (along with the 5th and 95th percentiles).

Figure 43: Probability of Failure for Wellheads Due to Ground Shaking
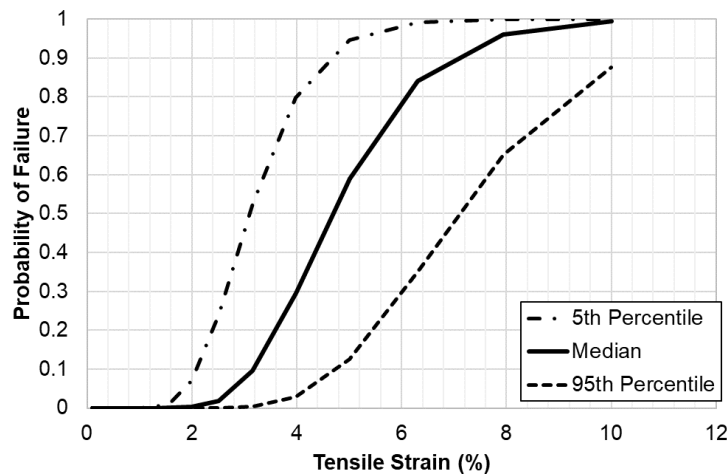
Source: Watson-Lamprey et al. (2022).

Pressure Vessels

For the pressure vessels, the critical component considered was the base of the pressure vessel. Two types of base connections were considered. The first represented the configuration of older pressure vessels, in which the base anchors were embedded in a

concrete footing and thus designed as a fully fixed connection. In this case, no elongation of the anchor would occur, and minimal base rotation was anticipated; consequently, the base of these pressure vessels was considered fixed. This case was labeled as "no stretch length." The second configuration was typical of newer pressure vessels. In this case, the anchors had a designed free stretch length of at least eight times the diameter of the anchor. This allowed the base to rotate; hence a nonlinear spring was incorporated in the model at the base of the vessel. The distribution of the probability of failure for pressure vessels with ground shaking is shown in Figure 44.

Figure 44: Probability of Failure for Pressure Vessels Due to Ground Shaking
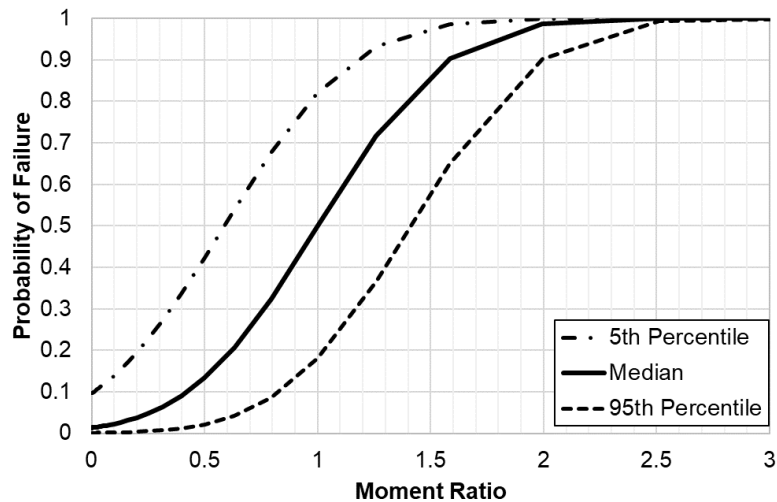
Source: Watson-Lamprey et al. (2022).

OpenSRA Graphical User Interface

The final component of *OpenSRA*, and the aspect that brings the backend calculations together, is the graphical user interface (GUI). Further information about the GUI and instructions on its use can be found in the User Manual.

The GUI consists of multiple tabs that follow the PBEE framework. The visualization tab shows the inputs (infrastructure, ground motion, faults, and base maps) and the system updates once the analysis is performed. Figure 45 depicts a representative view of the GUI, showing peak ground acceleration (PGA) contours of the South Napa (2014) ShakeMap and the publicly available transmission line database.

Figure 45: Screenshot of Graphical User Interface
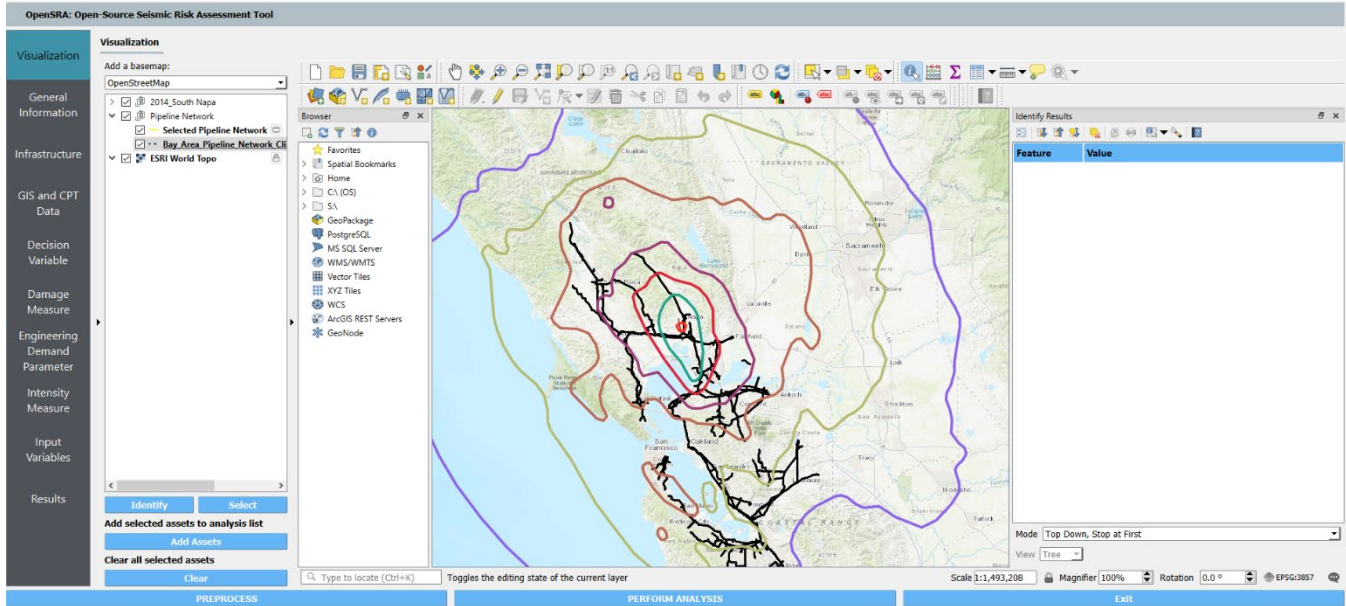
Example using the California Public Transmission Line Network with a USGS ShakeMap to predict the probability of failure of buried pipelines. The black lines depict the pipeline network and the colored lines are PGA contours of the ShakeMap.

Source: Zheng et al. (2023).

Project Metrics

Metric goals were established at the beginning of the project to monitor the successful progress of the project: website clicks, user workshop attendance, lab testing goals, and validation results. These metrics were associated with project exposure, interest and use of the software, and improvement of calculation methods.

This project met and exceeded these metrics. The interest in *OpenSRA* has grown; the number of project website clicks at the end of 2022 exceeded the goal by a factor of 33. The user workshop had around 80 registrations globally, with 31 in-person attendees; the in-person attendees benefitted from the hands-on software demonstrations. The number of lab test configurations exceeded the target goal by 30 percent. More information about knowledge transfer can be found in Kang et al. (2023). Validation of the software was conducted at four demonstration sites, and the *OpenSRA* results correlated well with documented observations after selected earthquakes or test earthquake events. More information about validation can be found in Bain et al. (2023).

CHAPTER 4:
Conclusion

The project developed new seismic risk assessment methods (demand and fragility functions of components) and implemented these into an open-source seismic risk assessment software called *OpenSRA*. The project was split into six task groups to assess the seismic demands imposed on gas infrastructure and the seismic fragility of individual components. The project teams provided guidance on how to calculate the probability of failure for different components of the gas system. This guidance was based on thorough literature reviews, discussions with utility owners, data analysis, laboratory testing, and finite element modeling.

The primary result of this project is the user-friendly open-source seismic risk software for gas pipelines and storage facilities called *OpenSRA*. It is available to the public through the PEER website. The *OpenSRA* software addresses several of the concerns associated with the ad hoc way current seismic risk assessments of gas pipelines and storage facilities are performed.

The performance-based earthquake engineering (PBEE) framework is implemented in the *OpenSRA* software through fragility curves that describe the seismic performance of key gas infrastructure components. The fragility curves were developed through state-of-the-art numerical modeling efforts based on how system components respond to earthquake hazards. The developed models incorporate comprehensive inventories of fault and pipeline crossings for California using the Quaternary Faults and Fold Database and incorporate geologic, subsurface, and topographic data required in updated earthquake hazard regional scale assessments.

The end products given for seismic demands included a fault-pipeline crossing database, methods to estimate primary and secondary fault displacement hazard, and methods to estimate geohazards induced by seismicity. Fragility curves were developed for buried pipelines, wells and caprocks, and aboveground gas infrastructure. These seismic demand and fragility elements were then used within the PBEE framework to estimate the probability of failure given an earthquake scenario. The developed *OpenSRA* software provides a user interface to allow utility owners to use all these calculations and findings to help prioritize mitigation efforts on their gas infrastructure.

To perform the calculations within *OpenSRA* in a timeframe that would be useful to the user, a novel method called polynomial chaos (PC) was implemented. This methodology can employ clearly defined means, aleatory variabilities, and epistemic uncertainties for each step of the PBEE risk method to deliver results rapidly. The use of PC over traditional Monte-Carlo sampling can easily improve the computation time by two to three orders of magnitude.

Improved models of earthquake-induced ground failure hazards (specifically liquefaction-induced lateral spreading and earthquake shaking-induced landslides) were developed to better capture these hazards at different levels of regional scale analysis. The uncertainty assigned to the ground failure hazard models at different regional scales are consistent with the information available in California at the state-wide, regional, and site-specific levels.

Experiments of pipe component system provided critical insights on their seismic performance. Advanced analysis of gas storage wells identified key response characteristics and insights on their seismic performance.

New sensing technologies were identified that can inform the risk models at the input, intermediate, and final output stages. The selected sensing technologies can be categorized into four main categories: 1) Remote sensing technologies, 2) Continuous monitoring technologies, 3) Inspection technologies, and 4) Leakage detection technologies. They were selected depending on the employed *OpenSRA* parameters, which included available geologic information and characteristics of the gas infrastructure.

The *OpenSRA* software helps utilities assess their infrastructure both pre- and post-earthquake. It also provides a consistent means for regulators to assess the seismic risk of the gas infrastructure in California. The software helps prioritize mitigation efforts of potentially vulnerable systems before an earthquake, using ground motion prediction equations and past earthquake ShakeMaps. After a seismic event occurs, *OpenSRA* also allows the end-user to assess potential leaks and breaks in the system to send out relief efforts quickly. This ability to not only prioritize mitigation efforts prior to an earthquake but also help prioritize larger potential breaks after an event allows utility owners to protect their constituents from potentially catastrophic failures. Along with this, these mitigation efforts reduce environmental impacts and allow for efficient planning and construction to occur on new gas infrastructure.

Given the focused timeframe of the project, and the lack of existing fragility curves currently available, this project focused on common infrastructure to be broadly applicable. *OpenSRA* would benefit from additional research to:

1. Integrate directly with the USGS for ShakeMap scenarios, so that *OpenSRA* can provide estimates of gas pipeline and storage facility damage after a major earthquake.

2. Develop and incorporate additional ground failure hazard demand models to enhance the capabilities of *OpenSRA*, to capture model uncertainty in its estimates.

3. Extend numerical models of soil-pipeline response to capture additional pipe systems and soil conditions for additional loading scenarios, such as distributed shear, to expand the number of conditions considered in *OpenSRA*.

4. Develop fragility functions for components not investigated in this research project, such as the performance of pipelines attached to bridges crossing rivers, to expand the capabilities of *OpenSRA*.

5. Perform additional pipe component and system testing to refine their fragility functions used in *OpenSRA,* to better capture the mechanical response of pipeline systems.

6. Allow for more flexibility in input datasets, so that users can more easily employ the different component and system datasets in their inventory.

7. Develop a more flexible output system, so users can choose what to receive and how to view their *OpenSRA* results.

8. Integrate network/flow analysis into infrastructure types that have upstream/ downstream dependencies, so that *OpenSRA* can better capture these system interaction relationships and their interdependent effects on performance.

9. Allow for more complex fault rupture scenarios (in addition to simple fault plane geometries), so that more realistic surface fault rupture ground deformation scenarios can be considered in *OpenSRA*.

10. Integrate other forms of natural hazards, such as rain-induced landslides, flooding, volcanic activity, winter weather, and wildfire, in addition to the earthquake hazard.

11. Further develop the backend of *OpenSRA* to make better use of computer resources for computational efficiency, to speed up *OpenSRA* calculations.

12. Develop cloud-based and server-based dissemination of datasets and updates or extend the application to be web-based for broader access of *OpenSRA* for owners, regulators, and consultants.

13. Install sensing technologies in a variety of gas infrastructure systems to evaluate their performance over an extended period, to enhance the reliability of the *OpenSRA* seismic risk assessments as this information is gathered over time.

14. Develop methodologies to optimize the updating of models using information from sensors on gas infrastructure performance, to provide a feedback loop to enhance the reliability of the models used in *OpenSRA* and better capture model uncertainty.

It is the hope of the research team to continue to expand the use of *OpenSRA* through additional research projects in the future.

GLOSSARY AND LIST OF ACRONYMS

Term	Definition
CEC	California Energy Commission
CPT	Cone penetration test
DFOS	Distributed fiber optic sensor
DM	Damage measure
DV	Decision variable
EDP	Engineering demand parameter
GUI	Graphical user interface
IM	Intensity measure
LDI	Lateral displacement index
NGA-West2	Next Generation Attenuation Relationships for Western US
OpenSRA	Open-source research-based seismic risk assessment tool
PBEE	Performance-based earthquake engineering
PC	Polynomial chaos
PEER	Pacific Earthquake Engineer Research (Center)
PGA	Peak ground acceleration
PSHA	Probabilistic seismic hazard analysis
TOUGH	Transport Of Unsaturated Groundwater and Heat
UCERF	Uniform California Earthquake Rupture Forecast
UGS	Underground storage
UNR	University of Nevada, Reno
VPV	Vertical pressure vessel
WSN	Wireless sensor network
WTP	Wellhead tree-pipeline (subsystem)

References

Abrahamson, N.A., Silva, W.J., and R. Kamai. 2014. Summary of the ASK14 Ground Motion Relation for Active Crustal Regions: Earthquake Spectra, v. 30, no. 3, p. 1025-1155.

Abrahamson, N. 2022. Personal Communication.

Bain, C., D. Hutabarat, J.D., Bray, N., Abrahamson, T.D., O'Rourke, and S. Lindvall. 2022. Performance-Based Earthquake Engineering Assessment Tool for Natural Gas Storage and Pipeline Systems, Task B - Enhanced Liquefaction and Ground Deformation Report. California Energy Commission.

Bain, C., T.D., O'Rourke, J., Bray, B., Zheng, D., Hutabarat, S., Lindvall, P., Jordan, T., Sasaki, K., Luu, Y., Zhang, W., Foxall, J., Rutqvist, D., McCallen, S., Elfass, T., Hutchinson, and E. Pantoli. 2023. Performance-Based Earthquake Engineering Assessment Tool for Natural Gas Storage and Pipeline Systems, Validation Report. California Energy Commission.

Boore, D.M., Stewart J.P., Seyhan, E., and G.M. Atkinson. 2014. NGA-West2 Equations for Prediction PGA, PGV, and 5%-Damped PSA for Shallow Crustal Earthquakes: Earthquake Spectra, v. 30, no. 3, p. 1057-1085.

Boulanger, R.W., and I.M. Idriss. 2016. CPT-based liquefaction triggering procedure. Journal of Geotechnical and Geoenvironmental Engineering, 142(2), 04015065-04015065.

Bray, J. D., and J. Macedo. 2019. Procedure for estimating shear-induced seismic slope displacement for shallow crustal earthquakes. Journal of Geotechnical and Geoenvironmental engineering, 145(12), 04019106.

Campbell, K.W., and Y. Bozorgnia. 2014. NGA-West2 Ground Motion Model for the Average Horizontal Component of PGA, PGV and 5% Damped Linear Acceleration Response Spectra: Earthquake Spectra, v. 30, no. 3, p. 1087-1115.

Cetin, K. O., H.T., Bilge, J., Wu, A.M., Kammerer, and R.B. Seed. 2009. Probabilistic model for the assessment of cyclically induced reconsolidation (volumetric) settlements. Journal of Geotechnical and Geoenvironmental Engineering, 135(3), 387.

Chiou, B.S., and R.R. Youngs. 2014. Update of the Chiou and Youngs NGA Model for the Average Horizontal Component of Peak Ground Motion and Response Spectra: Earthquake Spectra, v. 30, no. 3, p. 1117-1153.

Cornell, C.A. 1968. Engineering seismic risk analysis: Bulletin of the Seismological Society of America, v. 58, p. 1583–1606.

Elfass S., E., Pantoli, D., McCallen, and T.C. Hutchinson. 2023. Shake Table Testing of a Surface Natural Gas Piping Subsystem. A Report for the "Performance-based Earthquake Engineering Assessment Tool for Natural Gas Storage and Pipeline Systems" Project. PEER Report No. 2023/X. Pacific Earthquake Engineering Research Center, University of California, Berkeley, CA. Available at https://doi.org/X.

Field, E.H., Biasi, G.P., Bird, P., Dawson, T.E., Felzer, K.R., Jackson, D.D, Johnson, K.M., Jordan, T.H., Madden, C., Michael, A.J., Milner, K.R., Page, M.T., Parson, T., Powers, P.M., Shaw, B.E., Thatcher, W.R., Weldon, J.J. II, and Y. Zeng. 2013. Uniform California Earthquake Rupture Forecast, Version 3 (UCERF3) – The Time-Independent Model: U.S. Geological Survey Open-File Report 2013-1165.

FEMA (Federal Emergency Management Agency). 2020. Hazus 4.2 SP3 Technical Manual. Federal Emergency Management Agency. Available at https://www.fema.gov/sites/default/files/2020-10/fema_hazus_earthquake_technical_manual_4-2.pdf.

Grant, A., J., Wartman, and G. Abou-Jaoude. 2016. Multimodal method for coseismic landslide hazard assessment. Engineering Geology, 212, 146-160.

Holzer, T. L., T.E., Noce, and M.J. Bennett. 2011. Liquefaction Probability Curves for Surficial Geologic Deposits. Environmental and Engineering Geoscience, 17(1), 1–21. doi: 10.2113/gseegeosci.17.1.1.

Hutabarat, D., T.D., O'Rourke, J.D., Bray, C., Bain, and S. Lindvall. 2023. Performance-Based Earthquake Engineering Assessment Tool for Natural Gas Storage and Pipeline Systems, Underground Pipeline Fragilities. PEER Report No. 2023/X. Pacific Earthquake Engineering Research Center, University of California, Berkeley, CA. Available at https://doi.org/X.

Idriss, I.M., and R.W. Boulanger. 2008. Soil Liquefaction During Earthquakes. EERI Publication, Monograph MNO-12, Earthquake Engineering Research Institute, Oakland.

Idriss, I.M., and J.I. Sun. 1993. User's manual for SHAKE91: A computer program for conducting equivalent linear seismic response analyses of horizontally layered soil deposits. Center for Geotechnical Modeling, University of California, Davis.

Itasca Consulting Group. 2020. FLAC3D — Fast Lagrangian Analysis of Continua in Three-Dimensions, Ver. 7.0. Available at https://www.itascacg.com/software/FLAC3D.

Kang, G., J., Watson-Lamprey, and M. Largent. 2023. Performance-Based Earthquake Engineering Assessment Tool for Natural Gas Storage and Pipeline Systems, Knowledge Transfer Final Report. California Energy Commission.

Ku, C. S., C.H., Juang, C.W., Chang, and J. Ching. 2012. Probabilistic version of the Robertson and Wride method for liquefaction evaluation: development and application. Canadian Geotechnical Journal, 49(1), 27-44.

Lacour, M., and N. Abrahamson. 2021. Efficient Propagation of Epistemic Uncertainty for Probabilistic Seismic Hazard Analyses (PSHAs) Including Partial Correlation of Magnitude–Distance Scaling. Bulletin of the Seismological Society of America, 111(6), 3332-3340.

Lacour, M., and N. Abrahamson. 2023. Efficient Risk Calculation for Performance-Based Earthquake Engineering Distributed Systems. A Report for the "Performance-based Earthquake Engineering Assessment Tool for Natural Gas Storage and Pipeline Systems" Project. PEER Report No. 2023/X. Pacific Earthquake Engineering Research Center, University of California, Berkeley, CA. Available at https://doi.org/X.

Luu, K., P., Jordan, W., Foxall, and J. Rutqvist. 2023. Dynamic seismic analysis of wellbore integrity. A Report for the "Performance-based Earthquake Engineering Assessment Tool for Natural Gas Storage and Pipeline Systems" Project. PEER Report No. 2023/X. Pacific Earthquake Engineering Research Center, University of California, Berkeley, CA. Available at https://doi.org/X.

McKenna, F. 2011. OpenSees: A framework for earthquake engineering simulation. Computing in Science & Engineering 13(4):58–66. doi: 10.1109/MCSE.2011.66.

Moehle, J., and G.G. Deierlein. 2004. A framework methodology for performance-based earthquake engineering. 13th World Conference on Earthquake Engineering Proceedings (Vol. 679). Vancouver: WCEE, August 2004.

Moss, R. E., R.B., Seed, R.E., Kayen, J.P., Stewart, A., Der Kiureghian, and K.O. Cetin. 2006. CPT-based probabilistic and deterministic assessment of in situ seismic soil liquefaction potential. Journal of Geotechnical and Geoenvironmental Engineering, 132(8), 1032-1051.

Pantoli, E., T.C., Hutchinson, S.A., Elfass, and D.B. McCallen. 2022. Performance-Based Earthquake Engineering Assessment Tool for Natural Gas Storage and Pipeline Systems, Task D Final Report - Seismic Response of Pipeline and Gas Storage Surface Infrastructure. California Energy Commission.

Petersen, M. D., T. E. Dawson, R. Chen, T. Cao, C. J. Wills, D. P. Schwartz, and A. D. Frankel. 2011. Fault displacement hazard for strike-slip faults: Bulletin of the Seismological Society of America, v. 101, pp. 805–825.

Pruess, K., C. Oldenburg, and G. Moridis. 2011. TOUGH2 User's Guide, Version 2. LBNL-43134. Lawrence Berkeley National Laboratory, CA.

Robertson, P. K. 2009. Interpretation of cone penetration tests—a unified approach. Canadian geotechnical journal, 46(11), 1337-1355.

Robertson, P. K., and C.E. Wride. 1998. Evaluating cyclic liquefaction potential using the cone penetration test. Canadian geotechnical journal, 35(3), 442-459.

Rockpoint Gas Storage. n.d. Lodi. Available at https://www.rockpointgs.com/Businesses/Lodi. Accessed March 2021.

Rutqvist, J., T., Sasaki, L., Luu, P., Jordan, Y., Zhang, W., Foxall, J., Watson-Lamprey, M., Largent, and B. Zheng. 2022. Performance-Based Earthquake Engineering Assessment Tool for Natural Gas Storage and Pipeline Systems, Task C Final Report - Seismic Response of Wells and Caprocks. California Energy Commission.

Sasaki, T., P., Jordan, W., Foxall, and J. Rutqvist. 2023. Fragility of Wells due to Fault Shearing—The Impact of Fault Displacement on the Integrity of Natural Gas Storage Wells in California. A Report for the "Performance-based Earthquake Engineering Assessment Tool for Natural Gas Storage and Pipeline Systems" Project. PEER Report No. 2023/X. Pacific Earthquake Engineering Research Center, University of California, Berkeley, CA. Available at https://doi.org/X.

Smith M. 2009. Abaqus/Standard User's Manual, Version 6.9.

SoCalGas (Southern California Gas Company). 2016. How Underground Natural Gas Storage Works. Available at https://www.youtube.com/watch?v=3FSMpCazwUA. Accessed March 17, 2022.

Thompson, Stephen. 2021. Fault Displacement Hazard Characterization for OpenSRA. California Energy Commission.

USGS and CGS (United States Geological Survey and California Geological Survey). 2006. Quaternary Fault and Fold Database of the United States. Available at http://earthquake.usgs.gov/hazards/qfaults/. Accessed March 13, 2019.

Wald, D. J., B.C., Worden, V., Quitoriano, and K.L. Pankow. 2005. ShakeMap manual: technical manual, user's guide, and software guide (No. 12-A1).

Wang, C., P., Hubbard, T., Xu, and K. Soga. 2021. Performance-Based Earthquake Engineering Assessment Tool for Natural Gas Storage and Pipeline Systems, Task 4E Final Report – Sensor and Monitoring Technologies. California Energy Commission.

Watson-Lamprey, J., M., Largent, and B. Zheng. 2022. System Wide Natural Gas Infrastructure Response and Fragility Model. California Energy Commission.

Wells, D. L., and K. J. Coppersmith. 1994. New empirical relationships among magnitude, rupture length, rupture width, rupture area, and surface displacement: Bulletin of the Seismological Society of America, v. 84, pp. 974–1002.

Youd, T. L., and D.M. Perkins. 1978. Mapping liquefaction-induced ground failure potential. Journal of the Geotechnical Engineering Division, 104(4), 433-446.

Zhang, G., P.K., Robertson, and R.W.I. Brachman. 2002. Estimating Liquefaction-Induced Ground Settlements from CPT for Level Ground. Canadian Geotechnical Journal, 39(5), 1168–1180. doi: 10.1139/t02-047.

Zhang, Y., K., Ma, S., Song, M.B., Elam, G.A., Cook, and E.A. Park. 2004. Peroxisomal proliferator-activated receptor-γ coactivator-1α (PGC-1α) enhances the thyroid hormone induction of carnitine palmitoyltransferase I (CPT-Iα). Journal of Biological Chemistry, 279(52), 53963-53971.

Zhang, Y., P., Jordan, W., Foxall, and J. Rutqvist. 2023. Fragility Analysis Related to Caprock Leakage from Underground Gas Storage Reservoirs. A Report for the "Performance-based Earthquake Engineering Assessment Tool for Natural Gas Storage and Pipeline Systems" Project. PEER Report No. 2023/X. Pacific Earthquake Engineering Research Center, University of California, Berkeley, CA. Available at https://doi.org/X.

Zheng, B., M., Largent, T., Clifford, and J. Watson-Lamprey. 2023. Draft *OpenSRA* Report. California Energy Commission.

Zhu, J., L.G., Baise, and E.M. Thompson. 2017. An Updated Geospatial Liquefaction Model for Global Application. Bulletin of the Seismological Society of America, 107(3), 1365–1385. doi: 10.1785/0120160198.

Zhu, M., F., McKenna, and M.H. Scott. 2018. "OpenSeesPy: Python Library for the OpenSees Finite Element Framework." SoftwareX 7:6–11. doi: 10.1016/j.softx.2017.10.009.

Project Deliverables

The following project deliverables, including additional interim reports not listed below, are available upon request by submitting an email to pubs@energy.ca.gov. These deliverables can also be found at the project website https://www.peer.berkeley.edu/*OpenSRA*.

- Final Report
- *OpenSRA* Report
- *OpenSRA* Manual
- Fault Displacement Hazard Model Report
- Enhanced Regional Liquefaction and Ground Deformation Report
- Seismic Response of Wells and Caprocks Report
- Seismic Response of Pipeline and Gas Storage Surface Infrastructure Report
- Sensor and Monitoring Technologies Report
- Report of System Wide Natural Gas Infrastructure Response and Fragility Model
- Conceptual Design, Use Cases. and Development Plan Memorandum
- Validation Report
- Seismic Risk Analysis Tool *OpenSRA*